

CERN-PH-EP-2012-134

Submitted to: PLB

Measurement of the jet radius and transverse momentum dependence of inclusive jet suppression in lead-lead collisions at $\sqrt{s_{\text{NN}}} = 2.76$ TeV with the ATLAS detector

The ATLAS Collaboration

Abstract

Measurements of inclusive jet suppression in heavy ion collisions at the LHC provide direct sensitivity to the physics of jet quenching. In a sample of lead-lead collisions at $\sqrt{s_{\text{NN}}} = 2.76$ TeV corresponding to an integrated luminosity of approximately $7 \mu\text{b}^{-1}$, ATLAS has measured jets with a calorimeter system over the pseudorapidity interval $|\eta| < 2.1$ and over the transverse momentum range $38 < p_{\text{T}} < 210$ GeV. Jets were reconstructed using the anti- k_t algorithm with values for the distance parameter that determines the nominal jet radius of $R = 0.2, 0.3, 0.4$ and 0.5 . The centrality dependence of the jet yield is characterized by the jet “central-to-peripheral ratio,” R_{CP} . Jet production is found to be suppressed by approximately a factor of two in the 10% most central collisions relative to peripheral collisions. R_{CP} varies smoothly with centrality as characterized by the number of participating nucleons. The observed suppression is only weakly dependent on transverse momentum. A significant dependence of the R_{CP} on the jet radius is observed for jets with $p_{\text{T}} < 100$ GeV. These results provide the first direct measurement of inclusive jet suppression in heavy ion collisions and complement previous measurements of dijet transverse energy imbalance at the LHC.

Measurement of the jet radius and transverse momentum dependence of inclusive jet suppression in lead-lead collisions at $\sqrt{s_{\text{NN}}} = 2.76$ TeV with the ATLAS detector

The ATLAS Collaboration

Abstract

Measurements of inclusive jet suppression in heavy ion collisions at the LHC provide direct sensitivity to the physics of jet quenching. In a sample of lead-lead collisions at $\sqrt{s_{\text{NN}}} = 2.76$ TeV corresponding to an integrated luminosity of approximately $7 \mu\text{b}^{-1}$, ATLAS has measured jets with a calorimeter over the pseudorapidity interval $|\eta| < 2.1$ and over the transverse momentum range $38 < p_{\text{T}} < 210$ GeV. Jets were reconstructed using the anti- k_t algorithm with values for the distance parameter that determines the nominal jet radius of $R = 0.2, 0.3, 0.4$ and 0.5 . The centrality dependence of the jet yield is characterized by the jet “central-to-peripheral ratio,” R_{CP} . Jet production is found to be suppressed by approximately a factor of two in the 10% most central collisions relative to peripheral collisions. R_{CP} varies smoothly with centrality as characterized by the number of participating nucleons. The observed suppression is only weakly dependent on jet radius and transverse momentum. These results provide the first direct measurement of inclusive jet suppression in heavy ion collisions and complement previous measurements of dijet transverse energy imbalance at the LHC.

Keywords: LHC, ATLAS, heavy ion, jets

1. Introduction

Collisions of lead ions at the LHC are expected to create strongly interacting matter at the highest temperatures ever produced in the laboratory [1]. This matter may be deconfined with a high density of unscreened colour charges. High transverse momentum (p_{T}) quarks and gluons generated by hard-scattering processes have long been considered an important tool for probing the properties of the matter created in ultra-relativistic nuclear collisions. The energy loss of the partons propagating through the matter may provide direct sensitivity to the colour charge density and to the transport properties of the matter [2–4]. Indirect observations of substantial parton energy loss or “jet quenching” via suppressed single high- p_{T} hadron yields [5–8] and disappearance of the dijet contribution to di-hadron correlations [9, 10] have contributed to the conclusion that Au+Au collisions at RHIC produce a quark-gluon plasma [11, 12]. Observations of highly asymmetric dijets in central Pb+Pb collisions at the LHC [13–15] can be understood in

the context of “differential” jet quenching, where one parton produced from an initial hard-scattering loses significantly more energy than the other, possibly as a result of different path lengths of the partons in the matter [16]. However, the asymmetry is not sensitive to situations where the two jets in a dijet pair lose comparable amounts of energy, so other measurements are required to probe “inclusive” jet quenching.

The inclusive, per-event jet production rate provides such a measurement. Energy loss of the parent partons in the created matter may reduce or “suppress” the rate for producing jets at a given transverse momentum. Such energy loss is expected to increase with medium temperature and with increasing path length of the parton in the medium [17]. As a result, there should be more suppression in central Pb+Pb collisions, which have nearly complete overlap between the incident nuclei, and little or no suppression in peripheral collisions where the nuclei barely overlap. In the absence of energy loss, the jet production rate is expected to vary with Pb+Pb collision centrality approximately in

proportion to N_{coll} , the number of nucleon-nucleon collisions that take place during a single Pb+Pb collision. The jet suppression may be quantified using the central-to-peripheral ratio, R_{CP} , the ratio of the per-event jet yields divided by the number of nucleon-nucleon collisions in a given centrality bin to the same quantity in a peripheral centrality bin. The quantity, R_{CP} , has the advantage that potentially large systematic uncertainties, especially those arising from systematic errors on the jet energy scale, largely cancel when evaluating the ratios of jet spectra within the same data set. The variation of the suppression with jet transverse momentum and with collision centrality will depend both on the energy loss mechanism and on the experimental definition of the jet. In the case of radiative energy loss, jet energies can be reduced by greater “out-of-cone” radiation, which should be more severe for smaller jet radii [18–20]. Naively, collisional energy loss would result in a suppression that is independent of radius. However recent calculations suggest that collisional processes can also contribute to jet broadening [21]. A measurement of the radius dependence of jet suppression could further clarify the roles of radiative and collisional energy loss in jet quenching.

This Letter presents measurements of the inclusive jet R_{CP} in Pb+Pb collisions at a nucleon-nucleon centre-of-mass energy of $\sqrt{s_{\text{NN}}} = 2.76$ TeV using data collected during 2010 corresponding to an integrated luminosity of approximately $7 \mu\text{b}^{-1}$. Results are presented for jets reconstructed from energy deposits measured in the ATLAS calorimeters using the anti- k_t jet-finding algorithm [22]. The anti- k_t reconstruction was performed separately for four different values of the anti- k_t distance parameter, R , that specifies the nominal radius of the reconstructed jets, $R = 0.2, 0.3, 0.4$ and 0.5 . For the remainder of the Letter the term “radius” will refer to the distance parameter, R . The jet energy is functionally defined to be the total energy within the jet clustering algorithm above an uncorrelated underlying event. This jet definition may include medium response which is correlated with the jet. The underlying event contribution to each jet was subtracted on a per-jet basis, and the R_{CP} values were calculated after unfolding the jet spectra for distortions due to intrinsic jet resolution and underlying event fluctuations.

2. Experimental setup and trigger

The measurements presented here were performed using the ATLAS calorimeter, inner detector, trigger, and data acquisition systems [23]. The ATLAS calorimeter system consists of a liquid argon (LAr) electromagnetic (EM) calorimeter covering $|\eta| < 3.2$, a steel-scintillator sampling hadronic calorimeter covering $|\eta| < 1.7$, a LAr hadronic calorimeter covering $1.5 < |\eta| < 3.2$, and two LAr electromagnetic and hadronic forward calorimeters (FCal) covering $3.2 < |\eta| < 4.9^1$. The hadronic calorimeter granularities or cell sizes in $\Delta\eta \times \Delta\phi$ are 0.1×0.1 for $|\eta| < 2.5$ and 0.2×0.2 for $2.5 < |\eta| < 4.9^2$. The EM calorimeters are longitudinally segmented into three compartments with an additional pre-sampler layer. The EM calorimeter has a granularity that varies with layer and pseudorapidity, but which is generally much finer than that of the hadronic calorimeter. The middle sampling layer, which typically has the largest energy deposit in EM showers, has a $\Delta\eta \times \Delta\phi$ granularity of 0.025×0.025 over $|\eta| < 2.5$.

Charged particles associated with the calorimeter jets were measured over the pseudorapidity interval $|\eta| < 2.5$ using the inner detector [24]. The inner detector is composed of silicon pixel detectors in the innermost layers, followed by silicon microstrip detectors and a straw-tube tracker, all immersed in a 2 T axial magnetic field provided by a solenoid. Minimum bias Pb+Pb collisions were identified using measurements from the zero-degree calorimeters (ZDCs) and the minimum-bias trigger scintillator (MBTS) counters. The ZDCs are located symmetrically at $z = \pm 140$ m and cover $|\eta| > 8.3$. In Pb+Pb collisions the ZDCs primarily measure “spectator” neutrons – neutrons from the incident nuclei that do not interact hadronically. The MBTS measures charged particles over $2.1 < |\eta| < 3.9$ using two sets of counters placed at $z = \pm 3.6$ m. Events used in this analysis were selected for recording by the data acquisition system

¹ATLAS uses a right-handed coordinate system with its origin at the nominal interaction point (IP) in the centre of the detector and the z -axis along the beam pipe. The x -axis points from the IP to the centre of the LHC ring, and the y axis points upward. Cylindrical coordinates (r, ϕ) are used in the transverse plane, ϕ being the azimuthal angle around the beam pipe. The pseudorapidity is defined in terms of the polar angle θ as $\eta = -\ln \tan(\theta/2)$.

²An exception is the third (outermost) sampling layer, which has a segmentation of 0.2×0.1 up to $|\eta| = 1.7$.

using a logical or of ZDC and MBTS coincidence triggers. The MBTS coincidence required at least one hit in each side of the detector, and the ZDC coincidence trigger required the summed pulse height from each calorimeter to be above a threshold set below the single neutron peak.

3. Event selection and centrality definition

In the offline analysis, Pb+Pb collisions were required to have a primary vertex reconstructed from charged particle tracks with $p_T > 500$ MeV. The tracks were reconstructed from hits in the inner detector using the standard ATLAS track reconstruction algorithm [25] with settings optimized for the high hit density in heavy ion collisions [26]. Additional requirements of a ZDC coincidence, at least one hit in each MBTS counter, and a difference in times measured by the two sides of the MBTS detector of less than 3 ns were imposed. The combination of the ZDC and MBTS conditions and the primary vertex requirement efficiently eliminates both beam-gas interactions and photo-nuclear events [27]. These event selections yielded a total of 51 million minimum-bias Pb+Pb events. Previous studies [26] indicate that the combination of trigger and offline requirements select minimum-bias hadronic Pb+Pb collisions with an efficiency of $98 \pm 2\%$.

The centrality of Pb+Pb collisions was characterized by ΣE_T^{FCal} , the total transverse energy measured in the forward calorimeters. The distribution of ΣE_T^{FCal} was divided into intervals corresponding to successive 10% percentiles of the full centrality distribution after accounting for the missing 2% most peripheral events. A standard Glauber

Table 1: Results of Glauber model evaluation of $\langle N_{\text{part}} \rangle$ and associated errors, $\langle N_{\text{coll}} \rangle$, the N_{coll} ratios, R_{coll} , and fractional errors on R_{coll} for the centrality bins included in this analysis.

Centrality	$\langle N_{\text{part}} \rangle$	$\langle N_{\text{coll}} \rangle$	R_{coll}
0 – 10%	356 ± 2	1500 ± 115	57 ± 6
10 – 20%	261 ± 4	923 ± 68	35 ± 4
20 – 30%	186 ± 4	559 ± 41	21 ± 2
30 – 40%	129 ± 4	322 ± 24	12 ± 1
40 – 50%	86 ± 4	173 ± 14	6.5 ± 0.04
50 – 60%	53 ± 3	85 ± 8	3.2 ± 0.01
60 – 80%	23 ± 2	27 ± 4	1

Monte-Carlo analysis [28, 29] was used to estimate the average number of participating nucleons, $\langle N_{\text{part}} \rangle$, and the average number of nucleon-nucleon collisions, $\langle N_{\text{coll}} \rangle$, for Pb+Pb collisions in each of the centrality bins. The results are shown in Table 1. The R_{CP} measurements presented here use the 60–80% centrality bin as a common peripheral reference. The R_{CP} calculation requires the ratio, $R_{\text{coll}} \equiv \langle N_{\text{coll}} \rangle / \langle N_{\text{coll}}^{60-80} \rangle$, where $\langle N_{\text{coll}}^{60-80} \rangle$ is the average number of collisions in the 60–80% centrality bin. The R_{coll} uncertainties have been calculated by evaluating the changes in R_{coll} due to variations of the minimum-bias trigger efficiency, parameters of the Glauber calculation, and parameters in the modelling of the ΣE_T^{FCal} distribution [26]. The R_{coll} values and uncertainties are also reported in Table 1.

4. Monte Carlo samples

Three Monte Carlo (MC) samples [30] were used for the analysis in this Letter. A total of 1 million simulated minimum-bias Pb+Pb events were produced using version 1.38b of the HIJING event generator [31]. HIJING was run with default parameters except for the disabling of jet quenching. To simulate the effects of elliptic flow in Pb+Pb collisions, a parameterized centrality-, η - and p_T -dependent $\cos 2\phi$ modulation based on previous ATLAS measurements [26] was imposed on the particles after generation [32]. The detector response to the resulting HIJING events was evaluated using GEANT4 [33] configured with geometry and digitization parameters matching those of the 2010 Pb+Pb run.

A “MC overlay” data set, intended specifically for evaluating jet performance, was obtained by overlaying GEANT4-simulated $\sqrt{s_{\text{NN}}} = 2.76$ TeV pp hard-scattering events on the HIJING events described above. The pp events were obtained from the ATLAS MC09 tune [34] of the PYTHIA event generator [35]. One million PYTHIA hard-scattering events were generated for each of five intervals of \hat{p}_T , the transverse momentum of outgoing partons in the $2 \rightarrow 2$ hard-scattering, with boundaries 17, 35, 70, 140, 280 and 560 GeV. The pp events for each \hat{p}_T interval were overlaid on the same sample of HIJING events.

A smaller sample of “data overlay” events was produced by overlaying 150k GEANT4-simulated PYTHIA pp events onto 150k minimum-bias Pb+Pb data events recorded during the 2011 LHC

Pb+Pb run. Due to the different detector conditions in the 2010 and 2011 runs, the data overlay events cannot provide the corrections required for this analysis. However, they provide a valuable test of the accuracy of HIJING in describing the underlying event.

5. Jet reconstruction

Calorimeter jets were reconstructed from $\Delta\eta \times \Delta\phi = 0.1 \times 0.1$ towers using the anti- k_t algorithm [22] in four-vector recombination mode with anti- k_t distance parameters $R = 0.2, 0.3, 0.4$ and 0.5 . The tower energies were obtained by summing energies, calibrated at the electromagnetic energy scale [36], of all cells in all layers within the η and ϕ boundaries of the towers. Cells that span tower boundaries had their energy apportioned by the fraction of the cell contained within a given tower. The jet measurements presented here were obtained by performing the anti- k_t reconstruction on the towers prior to underlying event (UE) subtraction and then evaluating and subtracting the UE from each jet at the calorimeter cell level. The subtraction procedure calculates a per-event average UE energy density excluding contributions from jets and accounting for effects of elliptic flow modulation on the UE [37]. The UE estimation and subtraction was performed using a two-step procedure that was identical for all jet radii.

A first estimate of the UE average transverse energy density, $\rho_i(\eta)$, was evaluated in 0.1 intervals of η from all cells in each calorimeter layer, i , within the given η interval excluding those within “seed” jets. In the first subtraction step, the seeds are defined to be $R = 0.2$ jets containing at least one tower with $E_T > 3$ GeV and having a ratio of maximum tower transverse energy to average tower transverse energy, $E_T^{\max}/\langle E_T \rangle > 4$. Elliptic flow in Pb+Pb collisions can impose a $2v_2 \cos[2(\phi - \Psi_2)]$ modulation on the UE. Here, v_2 is the second coefficient in a Fourier decomposition of the azimuthal variation of the UE particle or energy density, and the event plane angle, Ψ_2 , determines the phase of the elliptic modulation. Standard techniques [26, 37] were used to measure Ψ_2 ,

$$\Psi_2 = \frac{1}{2} \tan^{-1} \left(\frac{\sum_k w_k E_{T_k} \sin(2\phi_k)}{\sum_k w_k E_{T_k} \cos(2\phi_k)} \right), \quad (1)$$

where k runs over cells in the FCal, ϕ_k represents the cell azimuthal angle, and w_k represent per-cell weights empirically determined to ensure a uniform Ψ_2 distribution. An η -averaged v_2 was measured separately for each calorimeter layer according to

$$v_{2i} = \frac{\sum_{j \in i} E_{T_j} \cos[2(\phi_j - \Psi_2)]}{\sum_{j \in i} E_{T_j}}, \quad (2)$$

where j runs over all cells in layer i . The UE-subtracted cell transverse energies were calculated according to

$$E_{T_j}^{\text{sub}} = E_{T_j} - A_j \rho_i(\eta_j) (1 + 2v_{2i} \cos[2(\phi_j - \Psi_2)]), \quad (3)$$

where E_{T_j} , η_j , ϕ_j and A_j represent the cell E_T , η and ϕ positions, and area, respectively for cells, j , in layer i . The kinematics for $R = 0.2$ jets generated in this first subtraction step were calculated via a four-vector sum of all (assumed massless) cells contained within the jets using the E_T values obtained from Eq. 3.

The second subtraction step starts with the definition of a new set of seeds using a combination of $R = 0.2$ jets from the first subtraction step with $E_T > 25$ GeV and track jets (defined below) with $p_T > 10$ GeV. Using this new set of seeds, a new estimate of the UE, $\rho'_i(\eta)$, was calculated excluding cells within $\Delta R = 0.4$ of the new seed jets, where $\Delta R = \sqrt{(\eta_{\text{cell}} - \eta_{\text{jet}})^2 + (\phi_{\text{cell}} - \phi_{\text{jet}})^2}$. New v_{2i} values, v'_{2i} , were also calculated excluding all cells within $\Delta\eta = 0.4$ of any of the new seed jets. This exclusion largely eliminates distortions of the calorimeter v_2 measurement in events containing high- p_T jets. The background subtraction was then applied to the original cell energies using Eq. 3 but with ρ_i and v_{2i} replaced by the new values, $\rho'_i(\eta)$ and v'_{2i} . New jet kinematics were obtained for all jet radii from a four-momentum sum of cells within the jets using the subtracted cell transverse energies. Jets generated in this second subtraction step having $E_T > 20$ GeV were recorded for subsequent analysis.

A correction of typically a few per cent was applied to the reconstructed jets to account for incomplete exclusion of towers within jets from the UE estimate due, for example, to differences in direction between the seeds and the final jets. This correction was validated by applying the full heavy ion jet reconstruction procedure to 2.76 TeV pp data

collected by ATLAS in March 2011. The reconstructed jets were compared, jet-by-jet, to those obtained from the pp jet reconstruction procedure. After this last correction for incomplete exclusion of jets from the background, the energy scales of the heavy ion and pp reconstruction procedures agreed to better than 1% for $E_T > 25$ GeV. A final correction depending on the jet η , E_T , and R was applied to obtain the correct hadronic energy scale for the reconstructed jets. The calibration constants were derived separately for the four jet radii using the same procedure applied to pp jet measurements [36].

In addition to the calorimeter jet reconstruction, track jets were reconstructed using the anti- k_t algorithm with $R = 0.4$ from charged tracks that have a good match to the primary vertex and that have $p_T > 4$ GeV. This threshold suppresses contributions of the UE to the track jet measurement. Specifically, an $R = 0.4$ track jet has an estimated likelihood of including an uncorrelated $p_T > 4$ GeV charged track of less than 4% in the 0–10% centrality bin. The single track reconstruction efficiency is $\approx 80\%$, approximately independent of centrality.

The fluctuating UE in Pb+Pb collisions can potentially produce reconstructed jets that do not originate from hard-scattering processes. In the remainder of this Letter such jets are referred to as “underlying event jets” or UE jets. A requirement that calorimeter jets match at least one track jet with $p_T > 7$ GeV or an EM cluster reconstructed from cells in the electromagnetic calorimeter [38] with $p_T > 7$ GeV was applied to exclude UE jets. The matching criterion for both track jets and EM clusters is that they lie within $\Delta R = 0.2$ of the jet. Applying this matching requirement provides a factor of about 50 rejection against UE jets while inducing an additional p_T -dependent inefficiency in the jet measurement. To accommodate the use of track jets in the UE jet rejection, the jet measurements presented here have been restricted to $|\eta| < 2.1$. The total number of jets above p_T thresholds of 40 GeV and 100 GeV in the data sample after event selection, UE jet rejection, and the $|\eta| < 2.1$ cut have been applied is shown in Table 2 for the most central and peripheral bins.

6. Performance of the jet reconstruction

The primary evaluation of the combined performance of the ATLAS detector and the analysis procedures described above in measuring un-

Table 2: Total number of jets in the data set with $p_T > 40$ GeV and $p_T > 100$ GeV in the 0–10% and 60–80% centrality bins after all event selection criteria, UE jet rejection, and the $|\eta| < 2.1$ cut have been applied.

R	$p_T > 40$ GeV		$p_T > 100$ GeV	
	0–10%	60–80%	0–10%	60–80%
0.2	112 333	8068	2308	162
0.3	287 153	12 629	3534	222
0.4	543 444	15 964	4974	277
0.5	710 158	18 573	7586	307

quenched jets was obtained using the MC overlay sample. In that MC sample, the kinematics of the reference PYTHIA generator-level jets (hereafter called “truth jets”) were reconstructed from PYTHIA final-state particles for $R = 0.2, 0.3, 0.4$ and 0.5 using the same techniques as applied in pp analyses [36]. Separately, the presence and approximate kinematics of HIJING-generated jets were obtained by running $R = 0.4$ anti- k_t reconstruction on final-state HIJING particles having $p_T > 4$ GeV. Accidental overlap of jets from unrelated hard-scattering processes may occur at non-negligible rates in the data due to the geometric enhancement of hard-scattering rates in Pb+Pb collisions. However, for the purposes of this Letter, the resulting combined jets are considered part of the physical jet spectrum and not a result of UE fluctuations. Then, to prevent the overlap of PYTHIA and HIJING jets from distorting the jet performance evaluated relative to PYTHIA truth jets, all PYTHIA truth jets within $\Delta R = 0.8$ of a $p_T > 10$ GeV HIJING jet were excluded from the analysis.

Following reconstruction of the overlaid MC events using the same algorithms that were applied to the data, PYTHIA truth jets passing the HIJING-jet exclusion were matched to the closest reconstructed jet of the same R value within $\Delta R = 0.2$. The resulting matched jets were used to evaluate the jet energy resolution (JER) and the jet energy scale (JES). The jet reconstruction efficiency was defined as the fraction of truth jets for which a matching reconstructed jet is found. The efficiency was evaluated both prior to (ε) and following (ε') UE jet rejection. For all three performance measurements, the different \hat{p}_T MC overlay samples were combined using a weighting based on the PYTHIA cross-sections for each \hat{p}_T range.

Figure 1 shows a summary of the ATLAS Pb+Pb jet reconstruction performance for $R = 0.2$ and

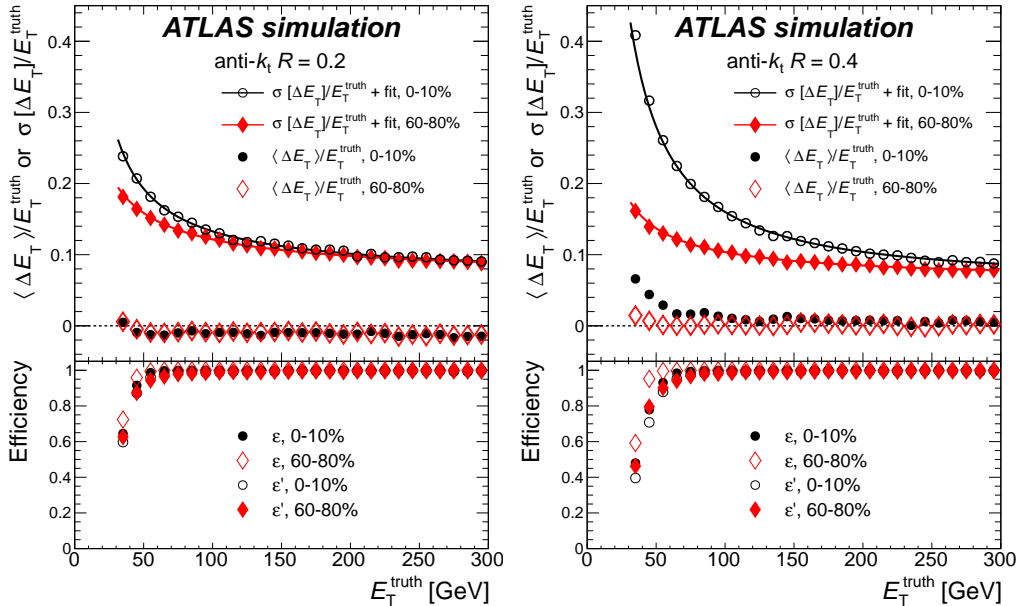


Figure 1: Results of MC evaluation of jet reconstruction performance in 0–10% and 60–80% collisions as a function of truth jet E_T for $R = 0.2$ (left) and $R = 0.4$ (right) jets. Top: jet energy resolution $\sigma[\Delta E_T]/E_T^{\text{truth}}$ and jet energy scale closure, $\langle \Delta E_T \rangle/E_T^{\text{truth}}$. Solid curves show parameterizations of the JER using Eq. 4. Bottom: Efficiencies, ϵ and ϵ' , for reconstructing jets before and after application of UE jet removal (see text for explanation), respectively.

$R = 0.4$ jets in central (0–10%) and peripheral (60–80%) collisions. The (fractional) JER was characterized by $\sigma[\Delta E_T]/E_T^{\text{truth}}$, where $\sigma[\Delta E_T]$ is the standard deviation of the $\Delta E_T \equiv E_T^{\text{rec}} - E_T^{\text{truth}}$ distribution and where E_T^{rec} and E_T^{truth} are the reconstructed and truth jet E_T values, respectively. The JES offset or “closure” was evaluated from the mean fractional energy shift, $\langle \Delta E_T \rangle/E_T^{\text{truth}}$.

The JER was found to be well described by a quadrature sum of three terms,

$$\frac{\sigma[\Delta E_T]}{E_T^{\text{truth}}} = \frac{a}{\sqrt{E_T^{\text{truth}}}} \oplus \frac{b}{E_T^{\text{truth}}} \oplus c, \quad (4)$$

where a and c represent the usual sampling and constant contributions to calorimeter resolution. The term containing b describes the contribution of underlying event fluctuations, which do not depend on jet E_T . Results of fitting the E_T dependence of the JER according to Eq. 4, using methods described below, are shown with curves in Fig. 1.

The jet reconstruction efficiency decreases with decreasing jet E_T for $E_T \lesssim 50$ GeV. The decrease starts at larger E_T and decreases more rapidly for larger jet radii and in more central collisions. The inefficiency results primarily from the finite JER

which causes jets with $E_T^{\text{truth}} > 20$ GeV to be measured with $E_T^{\text{rec}} < 20$ GeV. The UE jet rejection causes an additional loss of jets but in a manner that reduces the centrality dependence of the inefficiency.

The accuracy of the MC overlay studies described above was evaluated using the data overlay sample analyzed using the same procedures that were applied to the MC overlay sample. The analysis yielded results for the JER, JES, and efficiency consistent with the MC overlay sample, although the JER in the data overlay sample was found to be slightly better than in the MC overlay sample. The JES in the data overlay sample was found to agree between peripheral and central collisions to better than 1% for $R = 0.4$ jets, and the reconstruction efficiency was found to differ by less than 5% on the rise of the efficiency curve.

A data-driven check of the HIJING description of UE fluctuations was performed by evaluating distributions of EM-scale summed E_T in rectangular groups of towers within the interval $|\eta| < 2.8$. The groups were chosen to match the areas of jets used in this analysis: 3×4 and 7×7 for $R = 0.2$ and $R = 0.4$ jets, respectively. No attempt was made to exclude jets from the fluctuation analysis. The dis-

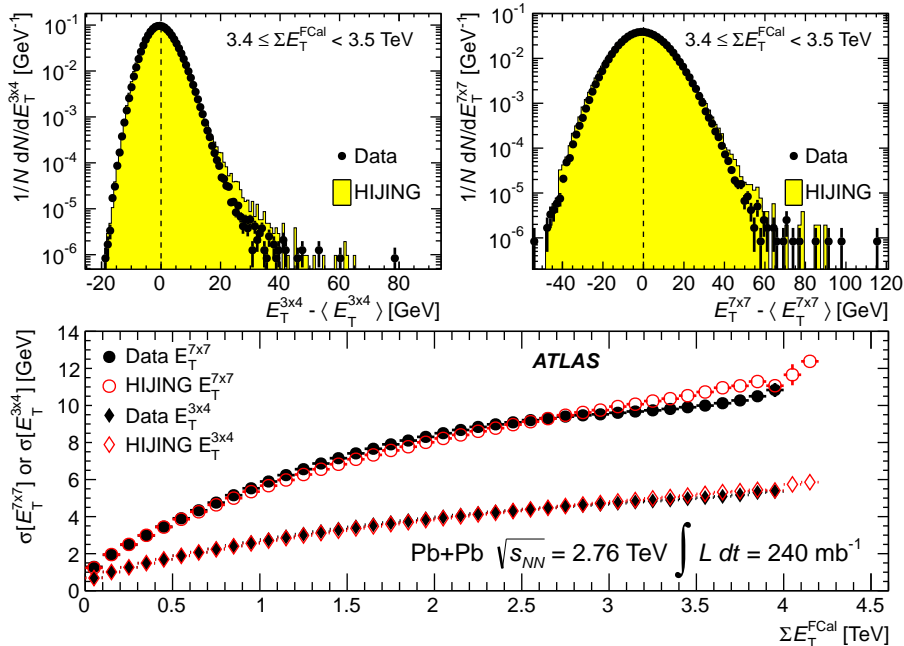


Figure 2: Top: Representative distributions of $E_T^{3 \times 4} - \langle E_T^{3 \times 4} \rangle$ (left) and $E_T^{7 \times 7} - \langle E_T^{7 \times 7} \rangle$ (right) (see text for definitions) for data (points) and MC (filled histogram) for Pb+Pb collisions with $3.4 \leq \Sigma E_T^{\text{FCal}} < 3.5$ TeV. The vertical lines indicate $E_T^{3 \times 4} - \langle E_T^{3 \times 4} \rangle = 0$ and $E_T^{7 \times 7} - \langle E_T^{7 \times 7} \rangle = 0$. Bottom: Standard deviations of the $E_T^{3 \times 4}$ and $E_T^{7 \times 7}$ distributions, $\sigma[E_T^{3 \times 4}]$ and $\sigma[E_T^{7 \times 7}]$, respectively, in data and HIJING MC sample as a function of ΣE_T^{FCal} .

tributions of $E_T^{3 \times 4}$ and $E_T^{7 \times 7}$, the ΣE_T for 3×4 and 7×7 groups of towers, are shown in Fig. 2 for a narrow range of ΣE_T^{FCal} , $3.4 \leq \Sigma E_T^{\text{FCal}} < 3.5$ TeV, that lies within the 0–1% centrality interval. These distributions have mean values, $\langle E_T^{3 \times 4} \rangle = 26$ GeV and $\langle E_T^{7 \times 7} \rangle = 105$ GeV, subtracted and, thus, in principle represent the distribution of the residual contributions of the UE to jet energies after subtraction. However, the high tails of the distributions can be attributed to the presence of jets, which are not part of the UE. The corresponding distributions obtained from the HIJING MC sample, but with $\langle E_T^{3 \times 4} \rangle$ and $\langle E_T^{7 \times 7} \rangle$ obtained from data, are shown in Fig. 2 with filled histograms.

The shapes of the MC and data distributions in Fig. 2 (top) are very similar, but the MC result slightly over-predicts the positive fluctuations for all collision centralities. In central collisions the MC result also slightly over-predicts the size of negative fluctuations. In contrast, for non-central collisions (not shown here) the data has a broader distribution of negative fluctuations than the MC sample. These observations are demonstrated by Fig. 2 (bottom) which shows the standard deviations of the $E_T^{3 \times 4}$ and $E_T^{7 \times 7}$ distributions, $\sigma[E_T^{3 \times 4}]$

and $\sigma[E_T^{7 \times 7}]$, as a function of ΣE_T^{FCal} , obtained from both the data and the MC sample. The data and MC distributions have similar trends, but the MC $\sigma[E_T^{3 \times 4}]$ and $\sigma[E_T^{7 \times 7}]$ values are larger in central collisions by 2.5% and 5%, respectively. In non-central collisions, the broader spectrum of negative fluctuations in the data causes $\sigma[E_T^{3 \times 4}]$ and $\sigma[E_T^{7 \times 7}]$ to exceed the corresponding quantity in the HIJING MC sample by approximately the same percentages.

Consistency between the results of the fluctuation analysis and the evaluation of the JER described above has been established by fitting the E_T dependence of the JER with the functional form given by Eq. 4 with fixed b values obtained from the fluctuation analysis. The b values for a given jet radius were determined by taking the standard deviation of the ΣE_T distribution for the corresponding tower group averaged over centrality and corrected to the hadronic energy scale. The resulting b values for $R = 0.2(0.4)$ jets are 5.62(12.45) GeV and 1.15(2.58) GeV for the 0–10% and 60–80% centrality bins respectively. The parameters a and c obtained from the fits are found to be independent of centrality within fit uncertainties, as expected, and to have values $a = 1.0(0.8)$, $c = 0.07(0.06)$ for

$R = 0.2(0.4)$ jets with E_T expressed in GeV. The accuracy of the fits in describing the E_T dependence of the JER is demonstrated by the curves showing results for $R = 0.2$ and $R = 0.4$ jets in Fig. 1.

The contribution of UE jets to the measured jet spectrum after UE jet rejection is estimated to be $\lesssim 3\%$ approximately independent of jet p_T for $40 < p_T < 60$ GeV and less than 1% for $p_T > 60$ GeV. This estimate was obtained by evaluating the rate of reconstructed jets in the HIJING MC sample which were not matched to HIJING truth jets and correcting for missing truth jets due to the $p_T > 4$ GeV requirement applied in the HIJING truth jet reconstruction.

7. Jet spectra and unfolding

Though jet reconstruction performance is naturally evaluated in terms of jet E_T , the physics measurements in this Letter were performed as a function of p_T directly calculated from the jet four-momentum. The typical masses of the jets are sufficiently small that $E_T \approx p_T$ holds over the range of measured p_T for all jet radii. The measured p_T spectra of reconstructed jets passing UE jet rejection and having $|\eta| < 2.1$ were evaluated for each centrality bin using logarithmic p_T bins spanning the range $38 < p_T < 210$ GeV. The correlations within and between p_T bins arising from multi-jet events were quantified by the covariance, C_{ij} , between the number of jets measured in two bins, i and j . The measured R_{CP} was calculated as

$$R_{CP}^{\text{meas}}(p_T)|_{\text{cent}} = \frac{1}{R_{\text{coll}}^{\text{cent}}} \left(\frac{N_{\text{jet}}^{\text{cent}}(p_T)}{N_{\text{evt}}^{\text{cent}}} \right) \left(\frac{N_{\text{jet}}^{60-80}(p_T)}{N_{\text{evt}}^{60-80}} \right), \quad (5)$$

where $N_{\text{jet}}^{\text{cent}}$ represents the measured jet yield in a given p_T and centrality bin, and $N_{\text{evt}}^{\text{cent}}$ and N_{evt}^{60-80} are the number of Pb+Pb collisions within the chosen and peripheral reference centrality intervals, respectively. Results for $R_{CP}^{\text{meas}}|_{0-10}$ obtained from the measured spectra are shown in Fig. 3 for $R = 0.2$ and $R = 0.4$ jets. The $R_{CP}^{\text{meas}}|_{0-10}$ for $R = 0.2$ jets is approximately equal to 0.5 over the measured p_T range. The $R_{CP}^{\text{meas}}|_{0-10}$ for $R = 0.4$ and $R = 0.2$ jets are consistent for $p_T > 120$ GeV, but at lower p_T , the $R = 0.4$ $R_{CP}^{\text{meas}}|_{0-10}$ increases relative to the $R = 0.2$ values. The difference between $R = 0.2$ and $R = 0.4$ $R_{CP}^{\text{meas}}|_{0-10}$ values can be mostly attributed

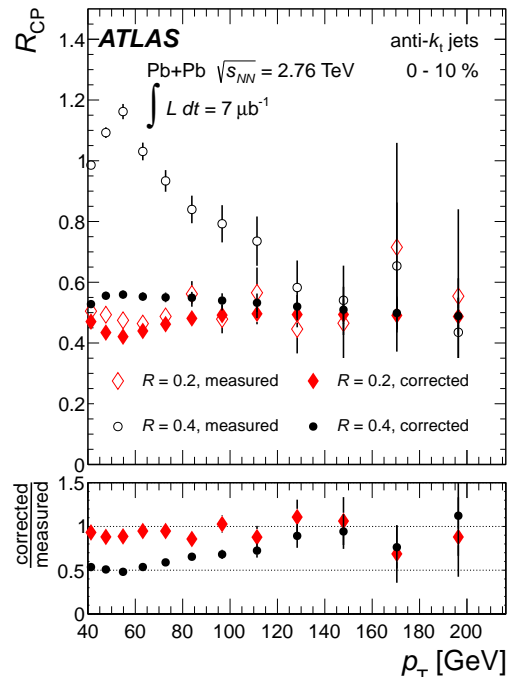


Figure 3: Top: Measured and corrected R_{CP} values for the 0–10% centrality bin as a function of jet p_T for $R = 0.4$ and $R = 0.2$ jets. Bottom: Ratio of corrected to measured R_{CP} values for both jet radii. The error bars on the points represent statistical uncertainties only.

to the difference in the size of the UE fluctuations for $R = 0.2$ and $R = 0.4$ jets shown in Fig. 1. The larger JER for $R = 0.4$ jets produces greater upward migration on the steeply falling jet p_T spectrum in central collisions than in peripheral collisions, thus enhancing the measured R_{CP} . The drop in the $R = 0.4$ $R_{CP}^{\text{meas}}|_{0-10}$ at low p_T is due to the decrease in jet reconstruction efficiency between 60–80% and 0–10% centrality bins which, as noted above, largely results from the worse JER in central collisions.

To remove the effects of the bin migration, the jet spectra were unfolded using the singular value decomposition (SVD) technique [39] as implemented in RooUnfold [40]. The MC overlay samples were used to populate a response matrix, \mathbf{A} , which describes the transformation of the true jet spectrum, \mathbf{x} , to the observed spectrum, \mathbf{b} , according to $\mathbf{b} = \mathbf{A}\mathbf{x}$. The truth and reconstructed jet p_T were obtained from the MC overlay sample using the methods described in Section 6, and 5, respectively, and the selection and matching of truth and

reconstructed jet pairs was performed as described in Section 6. Using the weighting method suggested in Ref. [39], the unfolded spectrum is expressed as a set of weights \mathbf{w} multiplying the input spectrum (x_{ini}) used to produce \mathbf{A} . The SVD method expresses the solution for \mathbf{w} in terms of a least-square minimization problem that includes a prescription for regularizing the amplification of statistical fluctuations of the data that would result from the direct inversion of \mathbf{A} . The regularization is controlled by a parameter τ such that contributions from singular values s_k of the unfolding matrix with $s_k < \tau$ are suppressed. Inclusion of the p_T -dependent reconstruction efficiency in the response was found to strongly affect the spectrum of singular values of the matrix defining the SVD problem, so the efficiency correction was applied separately following the unfolding. The spectrum of MC truth jets was reweighted to provide a smooth, power-law initial spectrum, $x_{\text{ini}} \propto \varepsilon'(p_T)/p_T^n$, where the power index was chosen to be $n = 5$. An analysis of the optimal regularization in the SVD unfolding following the methods of Ref. [39] indicated that a regularization parameter fixed by the fifth singular value ($\tau = s_5^2$) of the SVD matrix was appropriate for all centralities and all R values. The statistical uncertainties in the SVD unfolding due to statistical errors on the input spectrum were evaluated using the pseudo-experiment technique with 1000 separate stochastic variations of the input spectrum based on the full covariance matrix. The contributions of statistical fluctuations in the response matrix, \mathbf{A} , were similarly evaluated using an equal number of stochastic variations of the response matrix. The two contributions to the statistical uncertainty were combined in quadrature.

Potential biases in the unfolding procedure were evaluated using two different methods. Each unfolded spectrum was re-folded with its corresponding response matrix and compared to the measured spectrum for self-consistency. In general, regularization can introduce differences between re-folded and measured spectra on the scale of statistical uncertainties on the measured spectra, while over-regularization can produce larger, systematic differences. For all of the unfolded spectra, the re-folding procedure yielded a typical difference between measured and re-folded spectra comparable to the statistical uncertainties on the measured spectra. A separate check was performed by unfolding the reconstructed MC spectrum for each centrality bin and each jet radius and comparing to the original

MC truth jet spectrum. For this purpose, the MC data sets were divided in half and reconstructed spectra and response matrices were generated separately from each set. The unfolded and truth MC jet spectra typically agreed to better than 2%, though for the 0–10% centrality bin and for $R = 0.4$ and 0.5 jets, differences as large as 5% were observed in the lowest p_T bins. These differences are covered by the unfolding systematic uncertainties described below.

The corrected R_{CP} was evaluated according to

$$R_{\text{CP}}(p_T)|_{\text{cent}} = \frac{1}{R_{\text{coll}}^{\text{cent}}} \left(\frac{\frac{\tilde{N}_{\text{jet}}^{\text{cent}}(p_T)}{\varepsilon'^{\text{cent}} N_{\text{evt}}^{\text{cent}}}}{\frac{\tilde{N}_{\text{jet}}^{60-80}(p_T)}{\varepsilon'^{60-80} N_{\text{evt}}^{60-80}}} \right), \quad (6)$$

where \tilde{N}_{jet} represents the unfolded number of jets in the p_T bin, and $\varepsilon'^{\text{cent}}$ and ε'^{60-80} are the p_T -dependent jet reconstruction efficiencies after UE jet rejection for the indicated centrality bins. Figure 3 shows the comparison of the corrected and measured R_{CP} values as a function of jet p_T for $R = 0.2$ and $R = 0.4$ jets in the 0–10% centrality bin. The unfolding has little effect on the $R = 0.2$ R_{CP} due to the good energy resolution (relative to larger radii) for $R = 0.2$ jets even in central collisions. For the $R = 0.4$ jets, R_{CP} is reduced by a factor of about two at the lowest p_T values included in the analysis and is only slightly modified at the highest p_T . Because the unfolding provides a non-local mapping of the input jet p_T spectrum onto the unfolded spectrum, the statistical uncertainties in the unfolded spectra have significant correlations between bins, and there is not a direct relationship between the statistical errors in the input spectrum and the unfolded spectrum. The regularization of the unfolding also suppresses statistical fluctuations in the unfolded spectrum, but the statistical uncertainties in the measured spectrum also contributes to the systematic uncertainties from the unfolding procedure.

8. Systematic uncertainties

Systematic uncertainties in the R_{CP} measurement can arise due to errors on the jet energy scale (JES), the jet energy resolution (JER), jet finding efficiency, the unfolding procedure, and the R_{coll} values. Uncertainties in jet E_T and p_T are assumed to be equal (i.e. $\delta p_T = \delta E_T$). Uncertainties in the

JES and the JER influence the unfolding of the jet spectra. The resulting systematic uncertainties on the R_{CP} values (δR_{CP}^{sys}) were evaluated by producing new response matrices according to the procedures described below, generating unfolded spectra from these matrices, and calculating new R_{CP} values. The resulting changes in the R_{CP} values were taken to be estimates of δR_{CP}^{sys} . For uncertainties fully correlated in centrality, δR_{CP}^{sys} was evaluated by simultaneously varying the chosen centrality bin and the 60–80% bin, while for other uncertainties, the chosen centrality bin and 60–80% centrality bins were varied separately and the variations in R_{CP} combined in quadrature.

Overall JES uncertainties common to the different centrality bins cancel in the ratio of the spectra in R_{CP} , but centrality-dependent JES errors will produce a systematic shift in R_{CP} . Studies using the MC overlay sample discussed in Section 6 indicate a maximum difference in JES between the 0–10% and 60–80% centrality bins for the jet p_T range included in this analysis of 0.5%, 1%, 1.5% and 2.5% for $R = 0.2, 0.3, 0.4$ and 0.5 , respectively. Studies were also performed with the data overlay sample using an identical procedure as that applied to the MC overlay sample. The JES evaluated in the data overlay was found to agree between the 0–10% and 60–80% centrality bins to better than 1%, which is better than the agreement found in the MC overlay sample.

Independent evaluations of a possible centrality dependence of the calorimeter JES were performed by matching track and calorimeter jets in both the data and the MC overlay sample. The track jets provide a common reference for evaluating calorimeter jet response that is insensitive to the UE. The average calorimeter jet E_T was evaluated as a function of matching track jet p_T , $\langle E_T^{calo} \rangle(p_T^{trkjet})$, for different centrality bins. In the data, for $p_T^{trkjet} > 50$ GeV, the $\langle E_T^{calo} \rangle$ values were found to be consistent across all centrality bins to better than 3%. Accounting for a slight centrality dependence seen in the MC overlay sample, the 0–10% and 60–80% bins agree to 2%. For $p_T^{trkjet} < 50$ GeV, R - and centrality-dependent differences of up to 4% (for $R = 0.5$) are observed between data and MC overlay results for $\langle E_T^{calo} \rangle(p_T^{trkjet})$. This study provides a stringent constraint on changes in calorimeter response for jets affected by quenching and justifies the use of unquenched jets from PYTHIA in evaluating the jet performance and re-

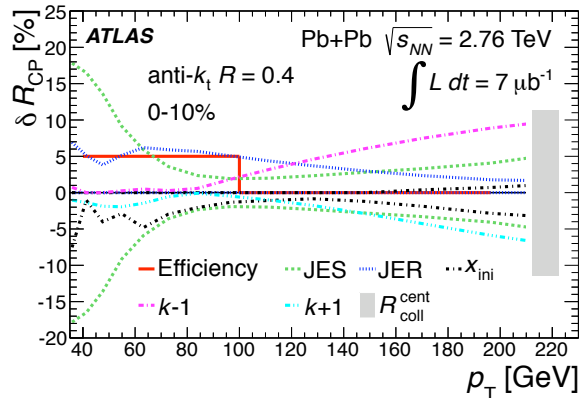


Figure 4: Contributions to the relative systematic uncertainty on the R_{CP} from various sources for the $R = 0.4$ anti- k_t jets in the 0–10% centrality bin. The $k \pm 1$ curves denote the uncertainty due to the choice of regularization parameter obtained by unfolding with the fourth and sixth singular values. A constant 5% systematic uncertainty on the jet reconstruction efficiency is assigned for $p_T < 100$ GeV only. The 11% uncertainty in the determination of R_{coll}^{cent} is indicated with a shaded box and is p_T -independent.

sponse matrices.

Based on the combination of the studies described above, the systematic uncertainties on the centrality dependence of the JES for the 0–10% centrality bin and for calorimeter jet $p_T > 70$ GeV were estimated to be 0.5%, 1%, 1.5% and 2.5%, respectively, for $R = 0.2, 0.3, 0.4$ and 0.5 jets. At lower p_T , the assigned systematic uncertainties increase linearly with decreasing p_T such that they double in size between 70 GeV and 38 GeV. For other centrality bins, the systematic errors on the centrality dependence of the JES decrease smoothly from central to peripheral collisions. The resulting δR_{CP}^{sys} values were evaluated using new response matrices generated by scaling the reconstructed p_T to account for the above-quoted JES uncertainties. The JES systematic uncertainty is assumed to be fully correlated between different centrality bins and different R values.

Systematic uncertainties in the JER due to inaccuracies in the MC description of the UE fluctuations were evaluated using results of the fluctuation analysis described above. The effects of those inaccuracies were evaluated by rescaling the per-jet $\Delta p_T \equiv p_T^{rec} - p_T^{truth}$ values obtained from the MC study by factors that cover the differences between data and MC result. For each centrality and jet radius, a modified value of the b parameter in Eq. 4

was evaluated and used to obtain new JER values, $\sigma'[\Delta E_T]$ from Eq. 4. Then a rescaled Δp_T was obtained from

$$\Delta p_T' = \Delta p_T \left(\frac{\sigma'}{\sigma} \right). \quad (7)$$

Since the discrepancies between the MC and the data were observed to be different for positive and negative fluctuations, the rescaling was applied separately for positive and negative Δp_T .

The ΣE_T values in the MC study were found to have larger positive fluctuations than those in the data for all centralities by approximately 2.5%, 2.5%, 5%, and 7.5% for $R = 0.2, 0.3, 0.4$ and 0.5 jets, respectively, so for positive Δp_T b was reduced by these percentages. For the 0–10% centrality bin, the negative fluctuations were also larger in the MC study than in the data by the same approximate percentages, so for central collisions the same, modified b value was used for negative Δp_T . For all other centrality bins, the negative fluctuations in the data were larger than in the MC by approximately twice the above-quoted percentages. Thus, for those centralities, the modified b values were obtained for negative Δp_T by increasing b by 5%, 5%, 10%, and 15%, respectively, for $R = 0.2, 0.3, 0.4$ and 0.5 jets.

New response matrices were generated using the calculated $\Delta p_T'$ values according to $p_T^{\text{rec}'} = p_T^{\text{truth}} + \Delta p_T'$, and these modified response matrices were used to estimate the JER systematic uncertainties following the procedure described above. The systematic uncertainty on the spectra due to the JER for the 0–10% centrality bin was taken to be one-sided as all evaluations indicate that the MC simulations slightly overestimate UE fluctuations. Asymmetric errors were obtained for the other centrality bins by applying the positive and negative ΔE_T scalings separately. The JER systematic uncertainties were assumed to be fully correlated between different jet R values but uncorrelated between different collision centralities, so the uncertainties on the spectra were combined in quadrature in evaluating $\delta R_{\text{CP}}^{\text{sys}}$. The conservative assumption that the JER uncertainties are fully uncorrelated between different centrality bins is based on the observation that the differences between data and the HIJING MC sample in the fluctuation analysis are not the same for all centralities.

The systematic uncertainties associated with the non-UE contributions to the JER (described by the a and c terms in Eq. 4) were evaluated following

procedures used by ATLAS in previous pp jet measurements [41]. New response matrices were generated by applying an additional stochastic smearing to the Δp_T values, and the systematic uncertainty was obtained by applying the procedure described above.

Systematic uncertainties on R_{CP} due to the unfolding were evaluated by changing the power index (n) in the functional form for x_{ini} by ± 0.5 and by varying the regularization parameter. The ± 0.5 change in the power law index was chosen because it produces a spectrum that changes relative to the default x_{ini} over the measured p_T range by a factor of about two – the typical suppression observed in central collisions. Thus, it covers the possibility that the true R_{CP} could increase to one or decrease to 0.25 over the measured p_T range. To evaluate the potential systematic uncertainty due to regularization, the unfolding was performed with regularization parameters obtained from the fourth and sixth singular values of the unfolding matrix, $\tau = s_4^2$ and $\tau = s_6^2$. Systematic uncertainties on the spectra were determined from the differences in the unfolded spectra. The resulting $\delta R_{\text{CP}}^{\text{sys}}$ values were obtained assuming that the regularization uncertainties on the two spectra are uncorrelated.

The systematic uncertainty on the efficiency correction was evaluated by comparing MC overlay and data overlay samples where differences less than 5% were observed on the “turn on” part of the efficiency curve. A 5% uncertainty due to the efficiency correction was applied to R_{CP} for $p_T < 100$ GeV in the four most central bins. To check for biases introduced by the UE jet rejection, the analysis was repeated with a significantly weakened rejection criterion in which jets were required to match a single track with $p_T > 4$ GeV. No significant differences in the R_{CP} were observed except for $p_T < 50$ GeV where differences as high as 4% were found. These differences can be attributed to the contribution of additional UE jets.

The different contributions to the total $\delta R_{\text{CP}}^{\text{sys}}$ are shown in Fig. 4 for $R = 0.4$ jets in the 0–10% centrality bin. The JES and x_{ini} uncertainties are approximately independent of p_T , while the JER uncertainty decreases with increasing p_T . The regularization uncertainty grows with increasing p_T due to the poorer statistical precision of the high- p_T points. The systematic uncertainties for the other radii show similar p_T and centrality dependence, with the JES and JER uncertainties increasing with jet radius as expected.

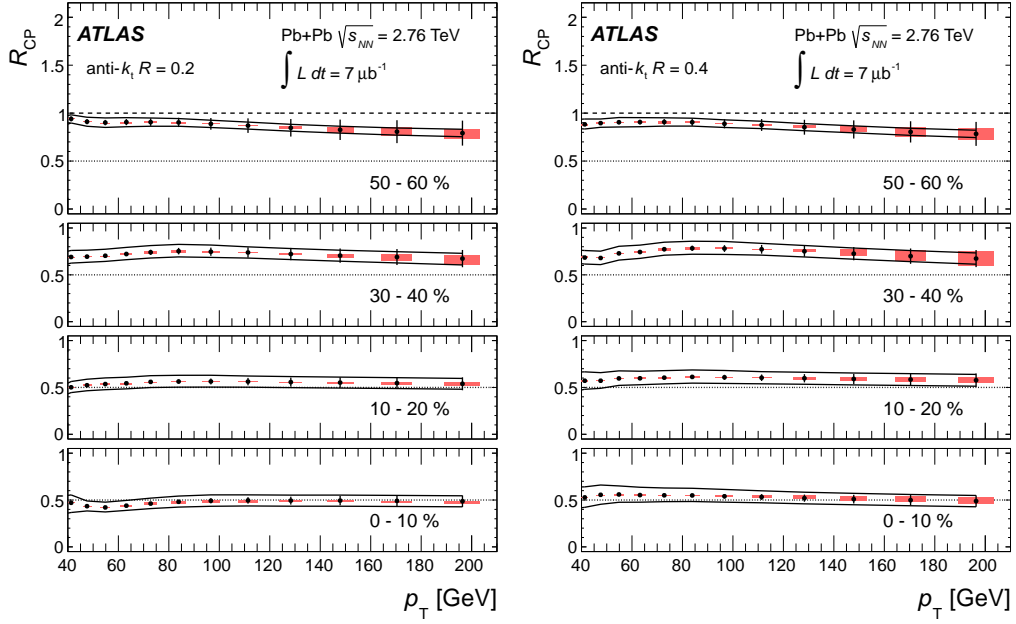


Figure 5: R_{CP} values as a function of jet p_T for $R = 0.2$ (left) and $R = 0.4$ (right) anti- k_t jets in four bins of collision centrality. The error bars indicate statistical errors from the unfolding, the shaded boxes indicate unfolding regularization systematic errors that are partially correlated between points. The solid lines indicate systematic errors that are fully correlated between all points. The horizontal width of the systematic error band is chosen for presentation purposes only. Dotted lines indicate $R_{CP} = 0.5$, and the dashed lines on the top panels indicate $R_{CP} = 1$.

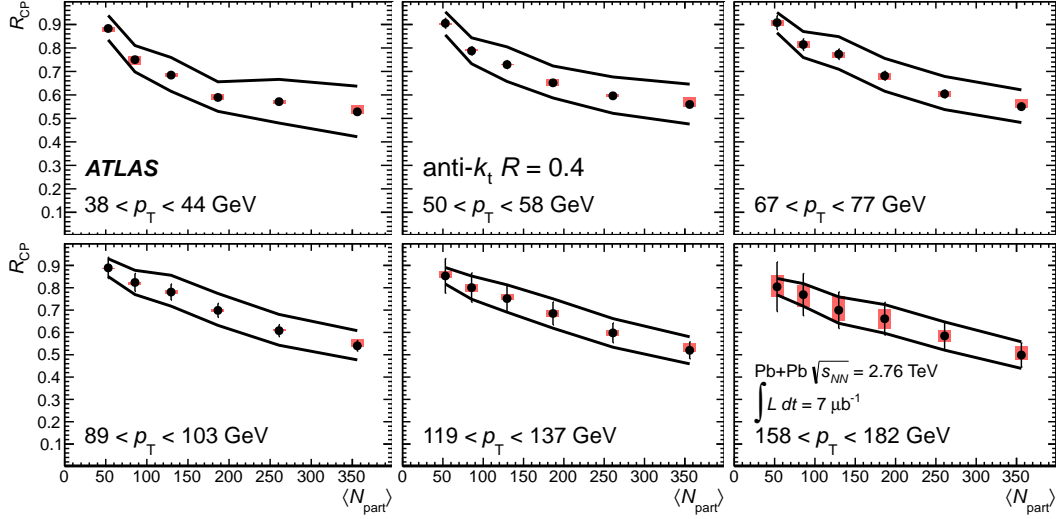


Figure 6: R_{CP} values as a function of N_{part} for $R = 0.4$ anti- k_t jets in six p_T bins. The error bars indicate statistical errors from the unfolding; the shaded boxes indicate point-to-point systematic errors that are only partially correlated. The solid lines indicate systematic errors that are fully correlated between all points. The horizontal errors indicate systematic uncertainties on N_{part} .

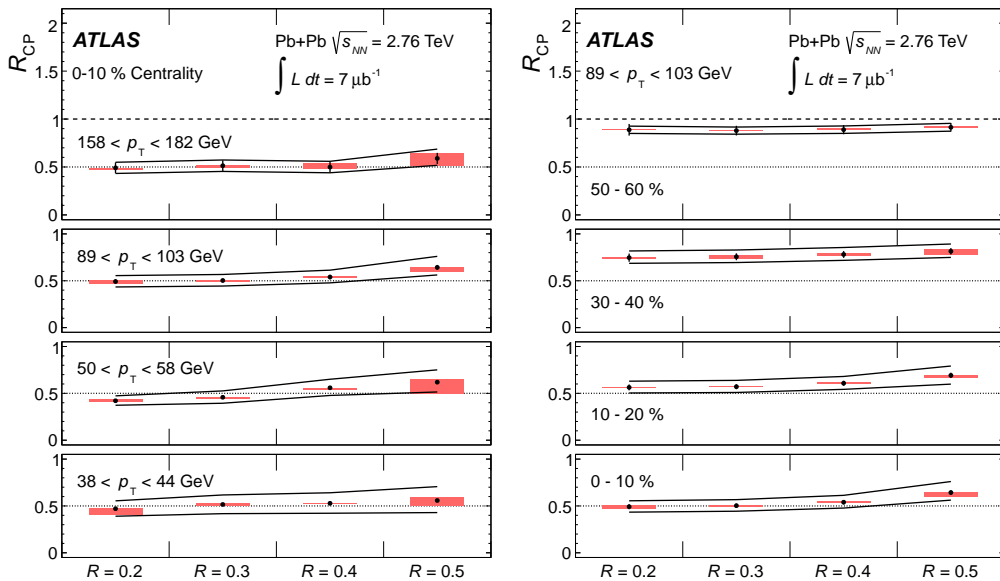


Figure 7: Left: R_{CP} in the 0–10% centrality bin as a function of jet radius for four bins of jet p_T . Right: R_{CP} as a function of jet radius for four centrality bins for the p_T interval $89 < p_T < 103$ GeV. The error bars indicate statistical errors from the unfolding; the shaded boxes indicate point-to-point systematic errors that are only partially correlated. The solid lines indicate systematic errors that are fully correlated between all points. The horizontal width of the systematic error band is chosen for presentation purposes only. Dotted lines indicate $R_{CP} = 0.5$, and the dashed lines on the top panels indicate $R_{CP} = 1$.

9. Results

Figure 5 shows the R_{CP} values obtained for $R = 0.2$ and $R = 0.4$ jets as a function of p_T in four bins of collision centrality with three different error contributions: statistical uncertainties, partially correlated systematic uncertainties, and fully correlated uncertainties. The R_{CP} values for all centralities and for both jet radii are observed to have at most a weak variation with p_T . For the 0–10% centrality bin the R_{CP} values for both jet radii show a factor of about two suppression in the $1/N_{\text{coll}}$ -scaled jet yield. For more peripheral collisions, R_{CP} increases at all jet p_T relative to central collisions, with the R_{CP} values reaching 0.9 for the 50–60% centrality bin. A more detailed evaluation of the centrality dependence of R_{CP} for $R = 0.4$ jets is presented in Fig. 6, which shows R_{CP} vs N_{part} for six jet p_T bins. R_{CP} decreases monotonically with increasing N_{part} for all p_T bins. The lower p_T bins, for which the data are more statistically precise, show a variation of R_{CP} with N_{part} that is most rapid at low N_{part} . Trends similar to those shown in Figs. 5 and 6 are observed for all jet radii.

The dependence of R_{CP} on jet radius is shown in Fig. 7 for the 0–10% centrality bin in four jet p_T intervals (left) and for different centrality bins in the

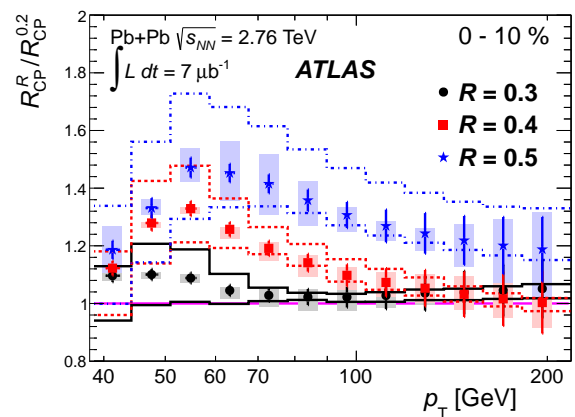


Figure 8: Ratios of R_{CP} values between $R = 0.3, 0.4$ and 0.5 jets and $R = 0.2$ jets as a function of p_T in the 0–10% centrality bin. The error bars show statistical uncertainties (see text). The shaded boxes indicate partially correlated systematic errors. The lines indicate systematic errors that are fully correlated between different p_T bins.

$89 < p_T < 103$ GeV bin (right). For this figure, the shaded boxes indicate the combined contribution of systematic uncertainties due to regularization, x_{ini} , and efficiency, which are only partially correlated between points. All other systematic er-

rors are fully correlated and are indicated by solid lines. The results in Fig. 7 show a weak variation of R_{CP} with R , that is nonetheless significant when taking into account the correlations in the errors between the different R values.

To demonstrate this conclusion more clearly, Fig. 8 shows the ratio of R_{CP} values between $R = 0.3, 0.4$ and 0.5 jets and $R = 0.2$ jets, $R_{\text{CP}}^R/R_{\text{CP}}^{0.2}$, as a function of p_{T} for the 0–10% centrality bin. When evaluating the ratio, there is significant cancellation between the correlated systematic uncertainties. Statistical correlations between the jet yields for the different radii were evaluated in the measured spectra and tracked through the unfolding procedure separately for the 0–10% and 60–80% centrality bins. Those correlations were then included when evaluating the statistical errors on $R_{\text{CP}}^R/R_{\text{CP}}^{0.2}$ shown in Fig. 8. The results in that figure indicate a significant dependence of R_{CP} on jet radius. For $p_{\text{T}} < 100$ GeV the $R_{\text{CP}}^R/R_{\text{CP}}^{0.2}$ values for both $R = 0.4$ and $R = 0.5$ differ from one beyond the statistical and systematic uncertainties. The deviation persists for $R = 0.5$ above 100 GeV. A similar, but weaker dependence is observed in the 10–20% centrality bin. In more peripheral bins, no significant radial dependence is observed. The differences between R_{CP} values for the different jet radii increase with decreasing p_{T} , except for the lowest two p_{T} bins. However, direct comparisons of R_{CP} between different jet radii at low p_{T} should be treated with care as the same jets measured using smaller radii will tend to appear in lower p_{T} bins than when measured with a larger radius.

10. Conclusions

This Letter presents results of measurements of the centrality dependence of jet suppression, characterized by the inclusive jet central-to-peripheral ratio, R_{CP} , in Pb+Pb collisions at 2.76 TeV per nucleon at the LHC. The measurements were performed over the p_{T} range $38 < p_{\text{T}} < 210$ GeV for anti- k_t jets of radii $R = 0.2, 0.3, 0.4$ and 0.5 . The inclusive jet yield is observed to be suppressed by a factor of about two in central collisions relative to peripheral collisions with at most a weak p_{T} dependence to the suppression. The suppression varies monotonically with collision centrality over the measured p_{T} range and for all jet radii. The R_{CP} at fixed p_{T} is observed to vary with jet radius increasing gradually from $R = 0.2$ to $R = 0.5$. That variation is most significant for $p_{\text{T}} < 100$ GeV

where more than a 30% variation is observed. These results provide the first direct measurement of inclusive jet suppression in heavy ion collisions. The substantial suppression of the jet yield observed at all p_{T} values complements the previous measurements of dijet transverse energy imbalance in Pb+Pb collisions at the LHC [13–15].

Acknowledgments

We thank CERN for the very successful operation of the LHC, as well as the support staff from our institutions without whom ATLAS could not be operated efficiently.

We acknowledge the support of ANPCyT, Argentina; YerPhI, Armenia; ARC, Australia; BMWF, Austria; ANAS, Azerbaijan; SSTC, Belarus; CNPq and FAPESP, Brazil; NSERC, NRC and CFI, Canada; CERN; CONICYT, Chile; CAS, MOST and NSFC, China; COLCIENCIAS, Colombia; MSMT CR, MPO CR and VSC CR, Czech Republic; DNRF, DNSRC and Lundbeck Foundation, Denmark; EPLANET and ERC, European Union; IN2P3-CNRS, CEA-DSM/IRFU, France; GNAS, Georgia; BMBF, DFG, HGF, MPG and AvH Foundation, Germany; GSRT, Greece; ISF, MINERVA, GIF, DIP and Benoziyo Center, Israel; INFN, Italy; MEXT and JSPS, Japan; CNRST, Morocco; FOM and NWO, Netherlands; RCN, Norway; MNiSW, Poland; GRICES and FCT, Portugal; MERYS (MECTS), Romania; MES of Russia and ROSATOM, Russian Federation; JINR; MSTD, Serbia; MSSR, Slovakia; ARRS and MVZT, Slovenia; DST/NRF, South Africa; MICINN, Spain; SRC and Wallenberg Foundation, Sweden; SER, SNSF and Cantons of Bern and Geneva, Switzerland; NSC, Taiwan; TAEK, Turkey; STFC, the Royal Society and Leverhulme Trust, United Kingdom; DOE and NSF, United States of America.

The crucial computing support from all WLCG partners is acknowledged gratefully, in particular from CERN and the ATLAS Tier-1 facilities at TRIUMF (Canada), NDGF (Denmark, Norway, Sweden), CC-IN2P3 (France), KIT/GridKA (Germany), INFN-CNAF (Italy), NL-T1 (Netherlands), PIC (Spain), ASGC (Taiwan), RAL (UK) and BNL (USA) and in the Tier-2 facilities worldwide.

References

- [1] Armesto, N. (Ed.). J. Phys. G 35 (2008) 054001. [arXiv:0711.0974](https://arxiv.org/abs/0711.0974).

- [2] X.-N. Wang, M. Gyulassy, M. Plumer. *Phys. Rev. D* 51 (1995) 3436–3446. [arXiv:hep-ph/9408344](#).
- [3] R. Baier, Y. L. Dokshitzer, A. H. Mueller, D. Schiff. *Phys. Rev. C* 58 (1998) 1706–1713. [arXiv:hep-ph/9803473](#).
- [4] M. Gyulassy, P. Levai, I. Vitev. *Phys. Rev. Lett.* 85 (2000) 5535–5538. [arXiv:nucl-th/0005032](#).
- [5] S. S. Adler, et al. *Phys. Rev. Lett.* 91 (2003) 072301. [arXiv:nucl-ex/0304022](#).
- [6] J. Adams, et al. *Phys. Rev. Lett.* 91 (2003) 172302. [arXiv:nucl-ex/0305015](#).
- [7] I. Arsene, et al. *Phys. Rev. Lett.* 91 (2003) 072305. [arXiv:nucl-ex/0307003](#).
- [8] B. B. Back, et al. *Phys. Rev. Lett.* 94 (2005) 082304. [arXiv:nucl-ex/0405003](#).
- [9] C. Adler, et al. *Phys. Rev. Lett.* 90 (2003) 082302. [arXiv:nucl-ex/0210033](#).
- [10] A. Adare, et al. *Phys. Rev. C* 78 (2008) 014901. [arXiv:0801.4545](#).
- [11] K. Adcox, et al. *Nucl. Phys. A* 757 (2005) 184–283. [arXiv:nucl-ex/0410003](#).
- [12] J. Adams, et al. *Nucl. Phys. A* 757 (2005) 102–183. [arXiv:nucl-ex/0501009](#).
- [13] ATLAS Collaboration. *Phys. Rev. Lett.* 105 (2010) 252303. [arXiv:1011.6182](#).
- [14] CMS Collaboration. *Phys. Rev. C* 84 (2011) 024906. [arXiv:1102.1957](#).
- [15] CMS Collaboration, CERN-PH-EP-2012-042 (2012). [arXiv:1202.5022](#).
- [16] J. D. Bjorken, Fermilab Preprint, FERMLAB-PUB-82-059-THY.
- [17] N. Armesto, B. Cole, C. Gale, W. A. Horowitz, P. Jacobs, et al., submitted to *Phys. Rev. C*. [arXiv:1106.1106](#).
- [18] I. Vitev, S. Wicks, B.-W. Zhang. *JHEP* 0811 (2008) 093. [arXiv:0810.2807](#).
- [19] I. Vitev, B.-W. Zhang. *Phys. Rev. Lett.* 104 (2010) 132001. [arXiv:0910.1090](#).
- [20] Y. He, I. Vitev, B.-W. Zhang. [arXiv:1105.2566](#).
- [21] G.-Y. Qin, B. Muller. *Phys.Rev.Lett.* 106 (2011) 162302. [arXiv:1012.5280](#), [doi:10.1103/PhysRevLett.106.189904](#), [10.1103/PhysRevLett.106.162302](#).
- [22] M. Cacciari, G. P. Salam, G. Soyez. *JHEP* 0804 (2008) 063. [arXiv:0802.1189](#).
- [23] ATLAS Collaboration. *JINST* 3 (2008) S08003.
- [24] ATLAS Collaboration. *Eur. Phys. J. C* 70 (2010) 787–821. [arXiv:1004.5293](#).
- [25] T. Cornelissen, M. Elsing, I. Gavrilenko, W. Liebig, E. Moyse, et al. *J. Phys. Conf. Ser.* 119 (2008) 032014.
- [26] ATLAS Collaboration. *Phys. Lett. B* 707 (2012) 330–348. [arXiv:1108.6018](#).
- [27] O. Djuvsland, J. Nystrand. *Phys. Rev. C* 83 (2010) 041901. [arXiv:1011.4908](#).
- [28] B. Alver, M. Baker, C. Loizides, P. Steinberg. [arXiv:0805.4411](#).
- [29] M. L. Miller, K. Reygers, S. J. Sanders, P. Steinberg. *Ann. Rev. Nucl. Part. Sci.* 57 (2007) 205–243. [arXiv:nucl-ex/0701025](#).
- [30] ATLAS Collaboration. *Eur. Phys. J. C* 70 (2010) 823–874. [arXiv:1005.4568](#).
- [31] X.-N. Wang, M. Gyulassy. *Phys. Rev. D* 44 (1991) 3501–3516.
- [32] M. Masera, G. Ortona, M. Poghosyan, F. Prino. *Phys. Rev. C* 79 (2009) 064909.
- [33] S. Agostinelli, et al. *Nucl. Instrum. Meth. A* 506 (2003) 250–303.
- [34] ATLAS Collaboration. *New J. Phys.* 13 (2010) 053033. [arXiv:1012.5104](#).
- [35] T. Sjostrand, S. Mrenna, P. Z. Skands. *JHEP* 0605 (2006) 026. [arXiv:hep-ph/0603175](#).
- [36] ATLAS Collaboration, submitted to *Eur. Phys. J. C*. [arXiv:1112.6426](#).
- [37] A. M. Poskanzer, S. Voloshin. *Phys. Rev. C* 58 (1998) 1671–1678. [arXiv:nucl-ex/9805001](#).
- [38] ATLAS Collaboration, CERN-OPEN-2008-20. [arXiv:0901.0512](#).
- [39] A. Hocker, V. Kartvelishvili. *Nucl. Instrum. Meth. A* 372 (1996) 469–481. [arXiv:hep-ph/9509307](#).
- [40] T. Abye, Proceedings of the PHYSTAT 2009 Workshop, CERN, Geneva, Switzerland, January 2011, CERN-2011-006, pp 313. [arXiv:1105.1160](#).
- [41] Atlas Collaboration. *Eur. Phys. J. C* 71 (2011) 1512. [arXiv:1009.5908](#).

The ATLAS Collaboration

G. Aad⁴⁸, B. Abbott¹¹¹, J. Abdallah¹¹, S. Abdel Khalek¹¹⁵, A.A. Abdelalim⁴⁹, O. Abdinov¹⁰, B. Abi¹¹², O.S. AbouZeid¹⁵⁸, H. Abramowicz¹⁵³, H. Abreu¹³⁶, B.S. Acharya^{164a,164b}, L. Adamczyk³⁷, D.L. Adams²⁴, T.N. Addy⁵⁶, J. Adelman¹⁷⁶, S. Adomeit⁹⁸, T. Adye¹²⁹, S. Aefsky²², J.A. Aguilar-Saavedra^{124b,a}, M. Agustoni¹⁶, M. Aharrouche⁸¹, S.P. Ahlen²¹, F. Ahles⁴⁸, A. Ahmad¹⁴⁸, M. Ahsan⁴⁰, G. Aielli^{133a,133b}, T. Akdogan^{18a}, T.P.A. Åkesson⁷⁹, G. Akimoto¹⁵⁵, A.V. Akimov⁹⁴, M.S. Alam¹, M.A. Alam⁷⁶, J. Albert¹⁶⁹, S. Albrand⁵⁵, M. Aleksa²⁹, I.N. Aleksandrov⁶⁴, C. Alexa^{25a}, G. Alexander¹⁵³, G. Alexandre⁴⁹, T. Alexopoulos⁹, M. Alhroob^{164a,164c}, M. Aliev¹⁵, G. Alimonti^{89a}, J. Alison¹²⁰, B.M.M. Allbrooke¹⁷, P.P. Allport⁷³, S.E. Allwood-Spiers⁵³, J. Almond⁸², A. Aloisio^{102a,102b}, R. Alon¹⁷², A. Alonso⁷⁹, B. Alvarez Gonzalez⁸⁸, M.G. Alvigi^{102a,102b}, K. Amako⁶⁵, C. Amelung²², A. Amorim^{124a,b}, N. Amram¹⁵³, C. Anastopoulos²⁹, L.S. Ancu¹⁶, N. Andari¹¹⁵, T. Andeen³⁴, C.F. Anders^{58b}, G. Anders^{58a}, K.J. Anderson³⁰, A. Andreazza^{89a,89b}, V. Andrei^{58a}, X.S. Anduaga⁷⁰, P. Anger⁴³, A. Angerami³⁴, F. Anghinolfi²⁹, A. Anisenkov¹⁰⁷, N. Anjos^{124a}, A. Annovi⁴⁷, A. Antonaki⁸, M. Antonelli⁴⁷, A. Antonov⁹⁶, J. Antos^{144b}, F. Anulli^{132a}, S. Aoun⁸³, L. Aperio Bella⁴, R. Apolle^{118,c}, G. Arabidze⁸⁸, I. Aracena¹⁴³, Y. Arai⁶⁵, A.T.H. Arce⁴⁴, S. Arfaoui¹⁴⁸, J-F. Arguin¹⁴, M. Arik^{18a}, A.J. Armbruster⁸⁷, O. Arnaez⁸¹, V. Arnal⁸⁰, C. Arnault¹¹⁵, A. Artamonov⁹⁵, G. Artoni^{132a,132b}, D. Arutinov²⁰, S. Asai¹⁵⁵, R. Asfandiyarov¹⁷³, S. Ask²⁷, B. Åsman^{146a,146b}, L. Asquith⁵, K. Assamagan²⁴, K. Augsten¹²⁷, M. Auresseau^{145a}, G. Avolio¹⁶³, R. Avramidou⁹, G. Azuelos^{93,d}, Y. Azuma¹⁵⁵, M.A. Baak²⁹, A.M. Bach¹⁴, H. Bachacou¹³⁶, K. Bachas²⁹, M. Backes⁴⁹, M. Backhaus²⁰, E. Badescu^{25a}, P. Bagnaia^{132a,132b}, S. Bahinipati², Y. Bai^{32a}, T. Bain¹⁵⁸, J.T. Baines¹²⁹, O.K. Baker¹⁷⁶, S. Baker⁷⁷, E. Banas³⁸, P. Banerjee⁹³, Sw. Banerjee¹⁷³, D. Banfi²⁹, A. Bangert¹⁵⁰, V. Bansal¹⁶⁹, H.S. Bansil¹⁷, L. Barak¹⁷², A. Barbaro Galtieri¹⁴, T. Barber⁴⁸, E.L. Barberio⁸⁶, D. Barberis^{50a,50b}, M. Barbero²⁰, T. Barillari⁹⁹, M. Barisonzi¹⁷⁵, T. Barklow¹⁴³, N. Barlow²⁷, B.M. Barnett¹²⁹, R.M. Barnett¹⁴, A. Baroncelli^{134a}, G. Barone⁴⁹, A.J. Barr¹¹⁸, F. Barreiro⁸⁰, J. Barreiro Guimarães da Costa⁵⁷, P. Barrillon¹¹⁵, R. Bartoldus¹⁴³, A.E. Barton⁷¹, V. Bartsch¹⁴⁹, R.L. Bates⁵³, L. Batkova^{144a}, J.R. Batley²⁷, A. Battaglia¹⁶, M. Battistin²⁹, F. Bauer¹³⁶, H.S. Bawa^{143,e}, S. Beale⁹⁸, T. Beau⁷⁸, P.H. Beauchemin¹⁶¹, R. Becherle^{50a}, P. Bechtel²⁰, H.P. Beck¹⁶, A.K. Becker¹⁷⁵, S. Becker⁹⁸, M. Beckingham¹³⁸, K.H. Becks¹⁷⁵, A.J. Beddall^{18c}, A. Beddall^{18c}, S. Bedikian¹⁷⁶, V.A. Bednyakov⁶⁴, C.P. Bee⁸³, M. Begel²⁴, S. Behar Harpaz¹⁵², M. Beimforde⁹⁹, C. Belanger-Champagne⁸⁵, P.J. Bell⁴⁹, W.H. Bell⁴⁹, G. Bella¹⁵³, L. Bellagamba^{19a}, F. Bellina²⁹, M. Bellomo²⁹, A. Belloni⁵⁷, O. Beloborodova^{107,f}, K. Belotskiy⁹⁶, O. Beltramello²⁹, O. Benary¹⁵³, D. Benchekroun^{135a}, K. Bendtz^{146a,146b}, N. Benekos¹⁶⁵, Y. Benhammou¹⁵³, E. Benhar Nocchioli⁴⁹, J.A. Benitez Garcia^{159b}, D.P. Benjamin⁴⁴, M. Benoit¹¹⁵, J.R. Bensinger²², K. Benslama¹³⁰, S. Bentvelsen¹⁰⁵, D. Berge²⁹, E. Bergeaas Kuutmann⁴¹, N. Berger⁴, F. Berghaus¹⁶⁹, E. Berglund¹⁰⁵, J. Beringer¹⁴, P. Bernat⁷⁷, R. Bernhard⁴⁸, C. Bernius²⁴, T. Berry⁷⁶, C. Bertella⁸³, F. Bertolucci^{122a,122b}, M.I. Besana^{89a,89b}, N. Besson¹³⁶, S. Bethke⁹⁹, W. Bhimji⁴⁵, R.M. Bianchi²⁹, M. Bianco^{72a,72b}, O. Biebel⁹⁸, S.P. Bieniek⁷⁷, K. Bierwagen⁵⁴, J. Biesiada¹⁴, M. Biglietti^{134a}, H. Bilokon⁴⁷, M. Bindi^{19a,19b}, S. Binet¹¹⁵, A. Bingul^{18c}, C. Bini^{132a,132b}, K.M. Black²¹, R.E. Blair⁵, J.-B. Blanchard¹³⁶, G. Blanchot²⁹, T. Blazek^{144a}, C. Blocker²², A. Blondel⁴⁹, W. Blum⁸¹, U. Blumenschein⁵⁴, G.J. Bobbink¹⁰⁵, V.B. Bobrovnikov¹⁰⁷, S.S. Bocchetta⁷⁹, A. Bocchi⁴⁴, C.R. Boddy¹¹⁸, M. Boehler⁴¹, J. Boek¹⁷⁵, N. Boelaert³⁵, J.A. Bogaerts²⁹, A. Bogdanchikov¹⁰⁷, C. Bohm^{146a}, V. Boisvert⁷⁶, T. Bold³⁷, N.M. Bolnet¹³⁶, M. Bomben⁷⁸, M. Bona⁷⁵, M. Boonekamp¹³⁶, S. Bordononi⁷⁸, C. Borer¹⁶, A. Borisov¹²⁸, G. Borissov⁷¹, I. Borjanovic^{12a}, M. Borri⁸², S. Borroni⁸⁷, V. Bortolotto^{134a,134b}, K. Bos¹⁰⁵, D. Boscherini^{19a}, M. Bosman¹¹, H. Boterenbrood¹⁰⁵, J. Bouchami⁹³, J. Boudreau¹²³, E.V. Bouhova-Thacker⁷¹, D. Boumediene³³, C. Bourdarios¹¹⁵, N. Bousson⁸³, A. Boveia³⁰, J. Boyd²⁹, I.R. Boyko⁶⁴, I. Bozovic-Jelisavcic^{12b}, J. Bracik¹⁷, A. Brandt⁷, G. Brandt¹¹⁸, O. Brandt⁵⁴, U. Bratzler¹⁵⁶, B. Brau⁸⁴, J.E. Brau¹¹⁴, S.F. Brazzale^{164a,164c}, B. Brelier¹⁵⁸, J. Bremer²⁹, K. Brendlinger¹²⁰, R. Brenner¹⁶⁶, S. Bressler¹⁷², D. Britton⁵³, F.M. Brochu²⁷, I. Brock²⁰, R. Brock⁸⁸, J. Bronner⁹⁹, G. Brooijmans³⁴, T. Brooks⁷⁶, W.K. Brooks^{31b}, G. Brown⁸², H. Brown⁷, P.A. Bruckman de Renstrom³⁸, D. Bruncko^{144b}, R. Bruneliere⁴⁸, S. Brunet⁶⁰, A. Bruni^{19a}, G. Bruni^{19a}, M. Bruschi^{19a}, T. Buanes¹³, Q. Buat⁵⁵, F. Bucci⁴⁹, J. Buchanan¹¹⁸, P. Buchholz¹⁴¹, R.M. Buckingham¹¹⁸, A.G. Buckley⁴⁵, S.I. Buda^{25a}, I.A. Budagov⁶⁴, B. Budick¹⁰⁸, V. Büscher⁸¹, L. Bugge¹¹⁷, O. Bulekov⁹⁶,

A.C. Bundock⁷³, M. Bunse⁴², H. Burckhart²⁹, S. Burdin⁷³, T. Burgess¹³, S. Burke¹²⁹, E. Busato³³,
 P. Bussey⁵³, C.P. Buszello¹⁶⁶, B. Butler¹⁴³, J.M. Butler²¹, C.M. Buttar⁵³, J.M. Butterworth⁷⁷,
 W. Buttlinger²⁷, S. Cabrera Urbán¹⁶⁷, D. Caforio^{19a,19b}, O. Cakir^{3a}, P. Calafiura¹⁴, G. Calderini⁷⁸,
 P. Calfayan⁹⁸, R. Calkins¹⁰⁶, L.P. Caloba^{23a}, D. Calvet³³, S. Calvet³³, R. Camacho Toro³³,
 D. Cameron¹¹⁷, L.M. Caminada¹⁴, S. Campana²⁹, M. Campanelli⁷⁷, V. Canale^{102a,102b}, F. Canelli^{30,g},
 A. Canepa^{159a}, J. Cantero⁸⁰, R. Cantrill⁷⁶, L. Capasso^{102a,102b}, M.D.M. Capeans Garrido²⁹, I. Caprini^{25a},
 M. Caprini^{25a}, D. Capriotti⁹⁹, M. Capua^{36a,36b}, R. Caputo⁸¹, R. Cardarelli^{133a}, T. Carli²⁹, G. Carlino^{102a},
 L. Carminati^{89a,89b}, B. Caron⁸⁵, S. Caron¹⁰⁴, E. Carquin^{31b}, G.D. Carrillo Montoya¹⁷³, J.R. Carter²⁷,
 J. Carvalho^{124a,h}, D. Casadei¹⁰⁸, M.P. Casado¹¹, M. Cascella^{122a,122b}, A.M. Castaneda Hernandez¹⁷³,
 E. Castaneda-Miranda¹⁷³, V. Castillo Gimenez¹⁶⁷, N.F. Castro^{124a}, P. Catastini⁵⁷, A. Catinaccio²⁹,
 J.R. Catmore²⁹, A. Cattai²⁹, G. Cattani^{133a,133b}, S. Caughron⁸⁸, D. Cavalli^{89a}, M. Cavalli-Sforza¹¹,
 V. Cavasinni^{122a,122b}, F. Ceradini^{134a,134b}, A.S. Cerqueira^{23b}, A. Cerri²⁹, L. Cerrito⁷⁵, F. Cerutti⁴⁷,
 S.A. Cetin^{18b}, A. Chafaq^{135a}, D. Chakraborty¹⁰⁶, I. Chalupkova¹²⁶, K. Chan², B. Chapleau⁸⁵,
 J.D. Chapman²⁷, E. Chareyre⁷⁸, D.G. Charlton¹⁷, V. Chavda⁸², C.A. Chavez Barajas²⁹, S. Cheatham⁸⁵,
 S. Chekanov⁵, S.V. Chekulaev^{159a}, G.A. Chelkov⁶⁴, M.A. Chelstowska¹⁰⁴, C. Chen⁶³, H. Chen²⁴,
 S. Chen^{32c}, X. Chen¹⁷³, Y. Chen³⁴, A. Cheplakov⁶⁴, R. Cherkaoui El Moursli^{135e}, V. Chernyatin²⁴,
 E. Cheu⁶, S.L. Cheung¹⁵⁸, L. Chevalier¹³⁶, G. Chiefari^{102a,102b}, L. Chikovani^{51a}, J.T. Childers²⁹,
 A. Chilingarov⁷¹, G. Chiodini^{72a}, A.S. Chisholm¹⁷, R.T. Chislett⁷⁷, M.V. Chizhov⁶⁴, G. Choudalakis³⁰,
 S. Chouridou¹³⁷, I.A. Christidi⁷⁷, D. Chromek-Burckhart²⁹, J. Chudoba¹²⁵, G. Ciapetti^{132a,132b},
 A.K. Ciftci^{3a}, R. Ciftci^{3a}, D. Cinca³³, V. Cindro⁷⁴, C. Ciocca^{19a,19b}, A. Cicio¹⁴, P. Cirkovic^{12b},
 M. Ciubancan^{25a}, A. Clark⁴⁹, P.J. Clark⁴⁵, J.C. Clemens⁸³, B. Clement⁵⁵, C. Clement^{146a,146b},
 Y. Coadou⁸³, M. Cobal^{164a,164c}, A. Cocco¹³⁸, J. Cochran⁶³, J.G. Cogan¹⁴³, J. Coggeshall¹⁶⁵,
 E. Cogneras¹⁷⁸, A.P. Colijn¹⁰⁵, N.J. Collins¹⁷, C. Collins-Tooth⁵³, J. Collot⁵⁵, T. Colombo^{119a,119b},
 G. Colon⁸⁴, P. Conde Muiño^{124a}, E. Coniavitis¹¹⁸, M.C. Conidi¹¹, S.M. Consonni^{89a,89b}, V. Consorti⁴⁸,
 S. Constantinescu^{25a}, G. Conti⁵⁷, F. Conventi^{102a,i}, M. Cooke¹⁴, B.D. Cooper⁷⁷, A.M. Cooper-Sarkar¹¹⁸,
 K. Copic¹⁴, T. Cornelissen¹⁷⁵, M. Corradi^{19a}, F. Corriveau^{85,j}, A. Cortes-Gonzalez¹⁶⁵, G. Cortiana⁹⁹,
 G. Costa^{89a}, M.J. Costa¹⁶⁷, D. Costanzo¹³⁹, T. Costin³⁰, D. Côté²⁹, L. Courneyea¹⁶⁹, G. Cowan⁷⁶,
 C. Cowden²⁷, B.E. Cox⁸², K. Cranmer¹⁰⁸, F. Crescioli^{122a,122b}, M. Cristinziani²⁰, G. Crosetti^{36a,36b},
 S. Crépe-Renaudin⁵⁵, C.-M. Cuciuc^{25a}, C. Cuenca Almenar¹⁷⁶, T. Cuhadar Donszelmann¹³⁹,
 M. Curatolo⁴⁷, C. Cuthbert¹⁵⁰, H. Czirr¹⁴¹, P. Czodrowski⁴³, Z. Czyczula¹⁷⁶, S. D'Auria⁵³,
 M. D'Onofrio⁷³, A. D'Orazio^{132a,132b}, C. Da Via⁸², W. Dabrowski³⁷, A. Dafinca¹¹⁸, T. Dai⁸⁷,
 C. Dallapiccola⁸⁴, M. Dam³⁵, D.S. Damiani¹³⁷, H.O. Danielsson²⁹, V. Dao⁴⁹, G. Darbo^{50a}, G.L. Darlea^{25b},
 W. Davey²⁰, T. Davidek¹²⁶, R. Davidson⁷¹, E. Davies^{118,c}, M. Davies⁹³, A.R. Davison⁷⁷, Y. Davygora^{58a},
 E. Dawe¹⁴², I. Dawson¹³⁹, R.K. Daya-Ishmukhametova²², K. De⁷, R. de Asmundis^{102a},
 S. De Castro^{19a,19b}, S. De Cecco⁷⁸, J. de Graat⁹⁸, N. De Groot¹⁰⁴, P. de Jong¹⁰⁵, H. De la Torre⁸⁰,
 F. De Lorenzi⁶³, L. de Mora⁷¹, L. De Nooij¹⁰⁵, D. De Pedis^{132a}, A. De Salvo^{132a}, U. De Sanctis^{164a,164c},
 A. De Santo¹⁴⁹, J.B. De Vivie De Regie¹¹⁵, W.J. Dearnaley⁷¹, R. Debbé²⁴, C. Debenedetti⁴⁵,
 B. Dechenaux⁵⁵, D.V. Dedovich⁶⁴, J. Degenhardt¹²⁰, C. Del Papa^{164a,164c}, J. Del Peso⁸⁰,
 T. Del Prete^{122a,122b}, T. Delemontex⁵⁵, M. Deliyergiyev⁷⁴, A. Dell'Acqua²⁹, L. Dell'Asta²¹,
 M. Della Pietra^{102a,i}, D. della Volpe^{102a,102b}, M. Delmastro⁴, P.A. Delsart⁵⁵, C. Deluca¹⁰⁵, S. Demers¹⁷⁶,
 M. Demichev⁶⁴, B. Demirköz^{11,k}, J. Deng¹⁶³, S.P. Denisov¹²⁸, D. Derendarz³⁸, J.E. Derkaoui^{135d},
 F. Derue⁷⁸, P. Dervan⁷³, K. Desch²⁰, E. Devetak¹⁴⁸, P.O. Deviveiros¹⁰⁵, A. Dewhurst¹²⁹, B. DeWilde¹⁴⁸,
 S. Dhaliwal¹⁵⁸, R. Dhullipudi^{24,l}, A. Di Ciaccio^{133a,133b}, L. Di Ciaccio⁴, A. Di Girolamo²⁹,
 B. Di Girolamo²⁹, A. Di Mattia¹⁷³, B. Di Micco²⁹, R. Di Nardo⁴⁷, A. Di Simone^{133a,133b},
 R. Di Sipio^{19a,19b}, M.A. Diaz^{31a}, E.B. Diehl⁸⁷, J. Dietrich⁴¹, T.A. Dietzsch^{58a}, S. Diglio⁸⁶,
 K. Dindar Yagci³⁹, J. Dingfelder²⁰, C. Dionisi^{132a,132b}, P. Dita^{25a}, S. Dita^{25a}, F. Dittus²⁹, F. Djama⁸³,
 T. Djobava^{51b}, M.A.B. do Vale^{23c}, T.K.O. Doan⁴, D. Dobos²⁹, E. Dobson^{29,m}, C. Doglioni⁴⁹,
 T. Doherty⁵³, J. Dolejsi¹²⁶, Z. Dolezal¹²⁶, T. Dohmae¹⁵⁵, M. Donadelli^{23d}, J. Donini³³, J. Dopke²⁹,
 A. Doria^{102a}, A. Dotti^{122a,122b}, M.T. Dova⁷⁰, A.D. Doxiadis¹⁰⁵, A.T. Doyle⁵³, M. Dris⁹, J. Dubbert⁹⁹,
 S. Dube¹⁴, E. Duchovni¹⁷², G. Duckeck⁹⁸, A. Dudarev²⁹, F. Dudziak⁶³, M. Dührssen²⁹, L. Duflot¹¹⁵,
 M-A. Dufour⁸⁵, M. Dunford²⁹, H. Duran Yildiz^{3a}, M. Dwuznik³⁷, M. Düren⁵², J. Ebke⁹⁸, S. Eckweiler⁸¹,
 K. Edmonds⁸¹, C.A. Edwards⁷⁶, N.C. Edwards⁵³, W. Ehrenfeld⁴¹, T. Eifert¹⁴³, G. Eigen¹³,

K. Einsweiler¹⁴, T. Ekelof¹⁶⁶, M. El Kacimi^{135c}, M. Ellert¹⁶⁶, S. Elles⁴, F. Ellinghaus⁸¹, K. Ellis⁷⁵,
 N. Ellis²⁹, J. Elmsheuser⁹⁸, M. Elsing²⁹, D. Emeljanov¹²⁹, R. Engelmann¹⁴⁸, A. Engl⁹⁸, A. Eppig⁸⁷,
 J. Erdmann⁵⁴, A. Ereditato¹⁶, D. Eriksson^{146a}, J. Ernst¹, M. Ernst²⁴, J. Ernwein¹³⁶, D. Errede¹⁶⁵,
 S. Errede¹⁶⁵, E. Ertel⁸¹, M. Escalier¹¹⁵, C. Escobar¹²³, X. Espinal Curull¹¹, B. Esposito⁴⁷,
 A.I. Etievre¹³⁶, E. Etzion¹⁵³, D. Evangelakou⁵⁴, H. Evans⁶⁰, L. Fabbri^{19a,19b}, C. Fabre²⁹,
 R.M. Fakhruddinov¹²⁸, S. Falciano^{132a}, Y. Fang¹⁷³, M. Fanti^{89a,89b}, A. Farbin⁷, A. Farilla^{134a}, J. Farley¹⁴⁸,
 T. Farooque¹⁵⁸, S. Farrell¹⁶³, S.M. Farrington¹¹⁸, P. Farthouat²⁹, P. Fassnacht²⁹, D. Fassouliotis⁸,
 B. Fathollahzadeh¹⁵⁸, A. Favareto^{89a,89b}, L. Fayard¹¹⁵, S. Fazio^{36a,36b}, R. Febbraro³³, P. Federic^{144a},
 O.L. Fedin¹²¹, W. Fedorko⁸⁸, M. Fehling-Kaschek⁴⁸, L. Felgioni⁸³, D. Fellmann⁵, C. Feng^{32d}, E.J. Feng³⁰,
 A.B. Fenyuk¹²⁸, J. Ferencei^{144b}, W. Fernando⁵, S. Ferrag⁵³, J. Ferrando⁵³, V. Ferrara⁴¹, A. Ferrari¹⁶⁶,
 P. Ferrari¹⁰⁵, R. Ferrari^{119a}, D.E. Ferreira de Lima⁵³, A. Ferrer¹⁶⁷, D. Ferrere⁴⁹, C. Ferretti⁸⁷,
 A. Ferretto Parodi^{50a,50b}, M. Fiascaris³⁰, F. Fiedler⁸¹, A. Filipčić⁷⁴, F. Filthaut¹⁰⁴, M. Fincke-Keeler¹⁶⁹,
 M.C.N. Fiolhais^{124a,h}, L. Fiorini¹⁶⁷, A. Firan³⁹, G. Fischer⁴¹, M.J. Fisher¹⁰⁹, M. Flechl⁴⁸, I. Fleck¹⁴¹,
 J. Fleckner⁸¹, P. Fleischmann¹⁷⁴, S. Fleischmann¹⁷⁵, T. Flick¹⁷⁵, A. Floderus⁷⁹, L.R. Flores Castillo¹⁷³,
 M.J. Flowerdew⁹⁹, T. Fonseca Martin¹⁶, A. Formica¹³⁶, A. Forti⁸², D. Fortin^{159a}, D. Fournier¹¹⁵, H. Fox⁷¹,
 P. Francavilla¹¹, S. Franchino^{119a,119b}, D. Francis²⁹, T. Frank¹⁷², S. Franz²⁹, M. Fraternali^{119a,119b},
 S. Fratina¹²⁰, S.T. French²⁷, C. Friedrich⁴¹, F. Friedrich⁴³, D. Froidevaux²⁹, J.A. Frost²⁷, C. Fukunaga¹⁵⁶,
 E. Fullana Torregrosa²⁹, B.G. Fulsom¹⁴³, J. Fuster¹⁶⁷, C. Gabaldon²⁹, O. Gabizon¹⁷², T. Gadfort²⁴,
 S. Gadomski⁴⁹, G. Gagliardi^{50a,50b}, P. Gagnon⁶⁰, C. Galea⁹⁸, E.J. Gallas¹¹⁸, V. Gallo¹⁶, B.J. Gallop¹²⁹,
 P. Gallus¹²⁵, K.K. Gan¹⁰⁹, Y.S. Gao^{143,e}, A. Gaponenko¹⁴, F. Garbersson¹⁷⁶, M. Garcia-Sciveres¹⁴,
 C. García¹⁶⁷, J.E. García Navarro¹⁶⁷, R.W. Gardner³⁰, N. Garelli²⁹, H. Garitaonandia¹⁰⁵, V. Garonne²⁹,
 C. Gatti⁴⁷, G. Gaudio^{119a}, B. Gaur¹⁴¹, L. Gauthier¹³⁶, I.L. Gavrilenko⁹⁴, C. Gay¹⁶⁸, G. Gaycken²⁰,
 E.N. Gazis⁹, P. Ge^{32d}, Z. Gecse¹⁶⁸, C.N.P. Gee¹²⁹, D.A.A. Geerts¹⁰⁵, Ch. Geich-Gimbel²⁰,
 K. Gellerstedt^{146a,146b}, C. Gemme^{50a}, A. Gemmel⁵³, M.H. Genest⁵⁵, S. Gentile^{132a,132b}, M. George⁵⁴,
 S. George⁷⁶, A. Gershon¹⁵³, N. Ghodbane³³, B. Giacobbe^{19a}, S. Giagu^{132a,132b}, V. Giakoumopoulou⁸,
 V. Giangiobbe¹¹, F. Gianotti²⁹, B. Gibbard²⁴, A. Gibson¹⁵⁸, S.M. Gibson²⁹, D. Gillberg²⁸,
 D.M. Gingrich^{2,d}, N. Giokaris⁸, M.P. Giordani^{164c}, R. Giordano^{102a,102b}, F.M. Giorgi¹⁵, P. Giovannini⁹⁹,
 P.F. Giraud¹³⁶, D. Giugni^{89a}, M. Giunta⁹³, B.K. Gjølsten¹¹⁷, L.K. Gladilin⁹⁷, C. Glasman⁸⁰, J. Glatzer⁴⁸,
 A. Glazov⁴¹, K.W. Glitza¹⁷⁵, G.L. Glonti⁶⁴, J.R. Goddard⁷⁵, J. Godfrey¹⁴², J. Godlewski²⁹, M. Goebel⁴¹,
 C. Goeringer⁸¹, C. Gössling⁴², S. Goldfarb⁸⁷, T. Golling¹⁷⁶, A. Gomes^{124a,b}, L.S. Gomez Fajardo⁴¹,
 R. Gonçalves⁷⁶, J. Goncalves Pinto Firmino Da Costa⁴¹, L. Gonella²⁰, S. González de la Hoz¹⁶⁷,
 G. Gonzalez Parra¹¹, M.L. Gonzalez Silva²⁶, S. Gonzalez-Sevilla⁴⁹, J.J. Goodson¹⁴⁸, L. Goossens²⁹,
 P.A. Gorbounov⁹⁵, H.A. Gordon²⁴, I. Gorelov¹⁰³, G. Gorfine¹⁷⁵, B. Gorini²⁹, E. Gorini^{72a,72b},
 A. Gorišek⁷⁴, E. Gornicki³⁸, B. Gosdzik⁴¹, A.T. Goshaw⁵, M.I. Gostkin⁶⁴, M. Goughri^{135a},
 D. Goujdami^{135c}, M.P. Goulette⁴⁹, A.G. Goussiou¹³⁸, C. Goy⁴, S. Gozpinar²², I. Grabowska-Bold³⁷,
 P. Grafström²⁹, K.-J. Grahn⁴¹, S. Grancagnolo¹⁵, V. Grassi¹⁴⁸, V. Gratchev¹²¹, N. Grau³⁴, H.M. Gray²⁹,
 J.A. Gray¹⁴⁸, E. Graziani^{134a}, O.G. Grebenyuk¹²¹, T. Greenshaw⁷³, Z.D. Greenwood^{24,l}, K. Gregersen³⁵,
 I.M. Gregor⁴¹, P. Grenier¹⁴³, J. Griffiths¹³⁸, A.A. Grillo¹³⁷, S. Grinstein¹¹, Y.V. Grishkevich⁹⁷,
 J.-F. Grivaz¹¹⁵, E. Gross¹⁷², J. Grosse-Knetter⁵⁴, J. Groth-Jensen¹⁷², K. Grybel¹⁴¹, D. Guest¹⁷⁶,
 C. Guicheney³³, S. Guindon⁵⁴, H. Guler^{85,n}, J. Gunther¹²⁵, B. Guo¹⁵⁸, J. Guo³⁴, P. Gutierrez¹¹¹,
 N. Guttman¹⁵³, O. Gutzwiller¹⁷³, C. Guyot¹³⁶, C. Gwenlan¹¹⁸, C.B. Gwilliam⁷³, A. Haas¹⁴³, S. Haas²⁹,
 C. Haber¹⁴, H.K. Hadavand³⁹, D.R. Hadley¹⁷, P. Haefner²⁰, S. Haider²⁹, Z. Hajduk³⁸, H. Hakobyan¹⁷⁷,
 D. Hall¹¹⁸, J. Haller⁵⁴, K. Hamacher¹⁷⁵, P. Hamal¹¹³, M. Hamer⁵⁴, A. Hamilton^{145b,o}, S. Hamilton¹⁶¹,
 L. Han^{32b}, K. Hanagaki¹¹⁶, K. Hanawa¹⁶⁰, M. Hance¹⁴, C. Handel⁸¹, P. Hanke^{58a}, J.R. Hansen³⁵,
 J.B. Hansen³⁵, J.D. Hansen³⁵, P.H. Hansen³⁵, P. Hansson¹⁴³, K. Hara¹⁶⁰, G.A. Hare¹³⁷, T. Harenberg¹⁷⁵,
 S. Harkusha⁹⁰, D. Harper⁸⁷, R.D. Harrington⁴⁵, O.M. Harris¹³⁸, J. Hartert⁴⁸, F. Hartjes¹⁰⁵, A. Harvey⁵⁶,
 S. Hasegawa¹⁰¹, Y. Hasegawa¹⁴⁰, S. Hassani¹³⁶, S. Haug¹⁶, M. Hauschild²⁹, R. Hauser⁸⁸, M. Havranek²⁰,
 C.M. Hawkes¹⁷, R.J. Hawkings²⁹, A.D. Hawkins⁷⁹, T. Hayakawa⁶⁶, T. Hayashi¹⁶⁰, D. Hayden⁷⁶,
 C.P. Hays¹¹⁸, H.S. Hayward⁷³, S.J. Haywood¹²⁹, S.J. Head¹⁷, V. Hedberg⁷⁹, L. Heelan⁷, S. Heim⁸⁸,
 B. Heinemann¹⁴, S. Heisterkamp³⁵, L. Helary⁴, C. Heller⁹⁸, M. Heller²⁹, S. Hellman^{146a,146b},
 D. Hellmich²⁰, C. Helsen¹¹, R.C.W. Henderson⁷¹, M. Henke^{58a}, A. Henrichs⁵⁴, A.M. Henriques Correia²⁹,
 S. Henrot-Versille¹¹⁵, C. Hensel⁵⁴, C.M. Hernandez⁷, Y. Hernández Jiménez¹⁶⁷, R. Herrberg¹⁵,

G. Herten⁴⁸, R. Hertenberger⁹⁸, L. Hervas²⁹, G.G. Hesketh⁷⁷, N.P. Hessey¹⁰⁵, E. Higón-Rodríguez¹⁶⁷, J.C. Hill²⁷, K.H. Hiller⁴¹, S. Hillert²⁰, S.J. Hillier¹⁷, I. Hinchliffe¹⁴, E. Hines¹²⁰, M. Hirose¹¹⁶, F. Hirsch⁴², D. Hirschbuehl¹⁷⁵, J. Hobbs¹⁴⁸, N. Hod¹⁵³, M.C. Hodgkinson¹³⁹, P. Hodgson¹³⁹, A. Hoecker²⁹, M.R. Hoferkamp¹⁰³, J. Hoffman³⁹, D. Hoffmann⁸³, M. Hohlfeld⁸¹, T. Holy¹²⁷, J.L. Holzbauer⁸⁸, T.M. Hong¹²⁰, L. Hooft van Huysduynen¹⁰⁸, S. Horner⁴⁸, J-Y. Hostachy⁵⁵, S. Hou¹⁵¹, A. Hoummada^{135a}, J. Howard¹¹⁸, J. Howarth⁸², I. Hristova¹⁵, J. Hrivnac¹¹⁵, T. Hryn'ova⁴, P.J. Hsu⁸¹, S.-C. Hsu¹⁴, Z. Hubacek¹²⁷, F. Hubaut⁸³, F. Huegging²⁰, A. Huettmann⁴¹, T.B. Huffman¹¹⁸, E.W. Hughes³⁴, G. Hughes⁷¹, M. Huhtinen²⁹, M. Hurwitz¹⁴, U. Husemann⁴¹, N. Huseynov^{64.p}, J. Huston⁸⁸, J. Huth⁵⁷, G. Iacobucci⁴⁹, G. Iakovidis⁹, I. Ibragimov¹⁴¹, L. Iconomidou-Fayard¹¹⁵, J. Idarraga¹¹⁵, P. Iengo^{102a}, O. Igonkina¹⁰⁵, Y. Ikegami⁶⁵, M. Ikeno⁶⁵, D. Iliadis¹⁵⁴, N. Ilic¹⁵⁸, T. Ince²⁰, P. Ioannou⁸, M. Iodice^{134a}, K. Iordanidou⁸, V. Ippolito^{132a,132b}, A. Irlles Quiles¹⁶⁷, C. Isaksson¹⁶⁶, M. Ishino⁶⁷, M. Ishitsuka¹⁵⁷, R. Ishmukhametov³⁹, C. Issever¹¹⁸, S. Istin^{18a}, A.V. Ivashin¹²⁸, W. Iwanski³⁸, H. Iwasaki⁶⁵, J.M. Izen⁴⁰, V. Izzo^{102a}, B. Jackson¹²⁰, J.N. Jackson⁷³, P. Jackson¹⁴³, M.R. Jaekel²⁹, V. Jain⁶⁰, K. Jakobs⁴⁸, S. Jakobsen³⁵, T. Jakoubek¹²⁵, J. Jakubek¹²⁷, D.K. Jana¹¹¹, E. Jansen⁷⁷, H. Jansen²⁹, A. Jantsch⁹⁹, M. Janus⁴⁸, G. Jarlskog⁷⁹, L. Jeanty⁵⁷, I. Jen-La Plante³⁰, P. Jenni²⁹, P. Jež³⁵, S. Jézéquel⁴, M.K. Jha^{19a}, H. Ji¹⁷³, W. Ji⁸¹, J. Jia¹⁴⁸, Y. Jiang^{32b}, M. Jimenez Belenguer⁴¹, S. Jin^{32a}, O. Jinnouchi¹⁵⁷, M.D. Joergensen³⁵, D. Joffe³⁹, M. Johansen^{146a,146b}, K.E. Johansson^{146a}, P. Johansson¹³⁹, S. Johnert⁴¹, K.A. Johns⁶, K. Jon-And^{146a,146b}, G. Jones¹⁷⁰, R.W.L. Jones⁷¹, T.J. Jones⁷³, P.M. Jorge^{124a}, K.D. Joshi⁸², J. Jovicevic¹⁴⁷, T. Jovin^{12b}, X. Ju¹⁷³, C.A. Jung⁴², R.M. Jungst²⁹, P. Jussel⁶¹, A. Juste Rozas¹¹, M. Kaci¹⁶⁷, A. Kaczmarska³⁸, P. Kadlecik³⁵, M. Kado¹¹⁵, H. Kagan¹⁰⁹, M. Kagan⁵⁷, E. Kajomovitz¹⁵², S. Kalinin¹⁷⁵, S. Kama³⁹, N. Kanaya¹⁵⁵, M. Kaneda²⁹, S. Kaneti²⁷, T. Kanno¹⁵⁷, V.A. Kantserov⁹⁶, J. Kanzaki⁶⁵, B. Kaplan¹⁷⁶, A. Kapliy³⁰, J. Kaplon²⁹, D. Kar⁵³, M. Karnevskiy⁴¹, V. Kartvelishvili⁷¹, A.N. Karyukhin¹²⁸, L. Kashif¹⁷³, G. Kasieczka^{58b}, R.D. Kass¹⁰⁹, A. Kastanas¹³, M. Kataoka⁴, Y. Kataoka¹⁵⁵, E. Katsoufis⁹, J. Katzy⁴¹, V. Kaushik⁶, K. Kawagoe⁶⁹, T. Kawamoto¹⁵⁵, G. Kawamura⁸¹, V.A. Kazanin¹⁰⁷, M.Y. Kazarinov⁶⁴, R. Keeler¹⁶⁹, R. Kehoe³⁹, M. Keil⁵⁴, G.D. Kekelidze⁶⁴, J.S. Keller¹³⁸, M. Kenyon⁵³, O. Kepka¹²⁵, N. Kerschen²⁹, B.P. Kerševan⁷⁴, S. Kersten¹⁷⁵, K. Kessoku¹⁵⁵, J. Keung¹⁵⁸, F. Khalil-zada¹⁰, H. Khandanyan¹⁶⁵, A. Khanov¹¹², D. Kharchenko⁶⁴, A. Khodinov⁹⁶, A. Khomich^{58a}, T.J. Khoo²⁷, G. Khoriauli²⁰, A. Khoroshilov¹⁷⁵, V. Khovanskiy⁹⁵, E. Khramov⁶⁴, J. Khubua^{51b}, H. Kim^{146a,146b}, S.H. Kim¹⁶⁰, N. Kimura¹⁷¹, O. Kind¹⁵, B.T. King⁷³, M. King⁶⁶, R.S.B. King¹¹⁸, J. Kirk¹²⁹, A.E. Kiryunin⁹⁹, T. Kishimoto⁶⁶, D. Kisieleska³⁷, T. Kittelmann¹²³, E. Kladiva^{144b}, M. Klein⁷³, U. Klein⁷³, K. Kleinknecht⁸¹, M. Klemetti⁸⁵, A. Klier¹⁷², P. Klimek^{146a,146b}, A. Klimentov²⁴, R. Klingenberg⁴², J.A. Klinger⁸², E.B. Klinkby³⁵, T. Klioutchnikova²⁹, P.F. Klok¹⁰⁴, E.-E. Kluge^{58a}, T. Kluge⁷³, P. Kluit¹⁰⁵, S. Kluth⁹⁹, E. Kneringer⁶¹, E.B.F.G. Knoops⁸³, A. Knue⁵⁴, T. Kobayashi¹⁵⁵, M. Kobel⁴³, M. Kocian¹⁴³, P. Kodys¹²⁶, K. Köneke²⁹, A.C. König¹⁰⁴, S. Koenig⁸¹, L. Köpke⁸¹, F. Koetsveld¹⁰⁴, P. Koevesarki²⁰, T. Koffas²⁸, E. Koffeman¹⁰⁵, L.A. Kogan¹¹⁸, S. Kohlmann¹⁷⁵, F. Kohn⁵⁴, Z. Kohout¹²⁷, T. Kohriki⁶⁵, T. Koi¹⁴³, H. Kolanoski¹⁵, V. Kolesnikov⁶⁴, I. Koletsou^{89a}, J. Koll⁸⁸, A.A. Komar⁹⁴, Y. Komori¹⁵⁵, T. Kondo⁶⁵, T. Kono^{41,q}, R. Konoplich^{108,r}, N. Konstantinidis⁷⁷, S. Koperny³⁷, K. Korcyl³⁸, K. Kordas¹⁵⁴, A. Korn¹¹⁸, A. Korol¹⁰⁷, I. Korolkov¹¹, E.V. Korolkova¹³⁹, V.A. Korotkov¹²⁸, O. Kortner⁹⁹, S. Kortner⁹⁹, V.V. Kostyukhin²⁰, S. Kotov⁹⁹, V.M. Kotov⁶⁴, A. Kotwal⁴⁴, C. Kourkoumelis⁸, V. Kouskoura¹⁵⁴, A. Koutsman^{159a}, R. Kowalewski¹⁶⁹, T.Z. Kowalski³⁷, W. Kozanecki¹³⁶, A.S. Kozhin¹²⁸, V. Kral¹²⁷, V.A. Kramarenko⁹⁷, G. Kramberger⁷⁴, M.W. Krasny⁷⁸, A. Krasznahorkay¹⁰⁸, J. Kraus⁸⁸, J.K. Kraus²⁰, S. Kreiss¹⁰⁸, F. Krejci¹²⁷, J. Kretschmar⁷³, N. Krieger⁵⁴, P. Krieger¹⁵⁸, K. Kroeninger⁵⁴, H. Kroha⁹⁹, J. Kroll¹²⁰, J. Kroseberg²⁰, J. Krstic^{12a}, U. Kruchonak⁶⁴, H. Krüger²⁰, T. Kruker¹⁶, N. Krumnack⁶³, Z.V. Krumshteyn⁶⁴, A. Kruth²⁰, T. Kubota⁸⁶, S. Kuday^{3a}, S. Kuehn⁴⁸, A. Kugel^{58c}, T. Kuhl⁴¹, D. Kuhn⁶¹, V. Kukhtin⁶⁴, Y. Kulchitsky⁹⁰, S. Kuleshov^{31b}, M. Kuna⁷⁸, J. Kunkle¹²⁰, A. Kupco¹²⁵, H. Kurashige⁶⁶, M. Kurata¹⁶⁰, Y.A. Kurochkin⁹⁰, V. Kus¹²⁵, E.S. Kuwertz¹⁴⁷, M. Kuze¹⁵⁷, J. Kvita¹⁴², R. Kwee¹⁵, A. La Rosa⁴⁹, L. La Rotonda^{36a,36b}, S. Lablak^{135a}, C. Lacasta¹⁶⁷, F. Lacava^{132a,132b}, H. Lacker¹⁵, D. Lacour⁷⁸, V.R. Lacuesta¹⁶⁷, E. Ladygin⁶⁴, R. Lafaye⁴, B. Laforge⁷⁸, T. Lagouri⁸⁰, S. Lai⁴⁸, E. Laisne⁵⁵, M. Lamanna²⁹, L. Lambourne⁷⁷, C.L. Lampen⁶, W. Lampl⁶, E. Lancon¹³⁶, U. Landgraf⁴⁸, M.P.J. Landon⁷⁵, V.S. Lang^{58a}, C. Lange⁴¹, A.J. Lankford¹⁶³, F. Lanni²⁴, K. Lantzschi¹⁷⁵, S. Laplace⁷⁸, C. Lapoire²⁰, J.F. Laporte¹³⁶, T. Lari^{89a}, A. Larner¹¹⁸, M. Lassnig²⁹, P. Laurelli⁴⁷, V. Lavorini^{36a,36b}, W. Lavrijsen¹⁴, P. Laycock⁷³, O. Le Dortz⁷⁸,

E. Le Guirriec⁸³, E. Le Menedeu¹¹, T. LeCompte⁵, F. Ledroit-Guillon⁵⁵, H. Lee¹⁰⁵, J.S.H. Lee¹¹⁶,
 S.C. Lee¹⁵¹, L. Lee¹⁷⁶, M. Lefebvre¹⁶⁹, M. Legendre¹³⁶, F. Legger⁹⁸, C. Leggett¹⁴, M. Lehmacher²⁰,
 G. Lehmann Miotto²⁹, X. Lei⁶, M.A.L. Leite^{23d}, R. Leitner¹²⁶, D. Lellouch¹⁷², B. Lemmer⁵⁴,
 V. Lendermann^{58a}, K.J.C. Leney^{145b}, T. Lenz¹⁰⁵, B. Lenzi²⁹, K. Leonhardt⁴³, S. Leontsinis⁹, F. Lepold^{58a},
 C. Leroy⁹³, J-R. Lessard¹⁶⁹, C.G. Lester²⁷, C.M. Lester¹²⁰, J. Levêque⁴, D. Levin⁸⁷, L.J. Levinson¹⁷²,
 A. Lewis¹¹⁸, G.H. Lewis¹⁰⁸, A.M. Leyko²⁰, M. Leyton¹⁵, B. Li⁸³, H. Li^{173,s}, S. Li^{32b,t}, X. Li⁸⁷,
 Z. Liang^{118,u}, H. Liao³³, B. Liberti^{133a}, P. Lichard²⁹, M. Lichtnecker⁹⁸, K. Lie¹⁶⁵, W. Liebig¹³,
 C. Limbach²⁰, A. Limosani⁸⁶, M. Limper⁶², S.C. Lin^{151,v}, F. Linde¹⁰⁵, J.T. Linnemann⁸⁸, E. Lipeles¹²⁰,
 A. Lipniacka¹³, T.M. Liss¹⁶⁵, A. Lister⁴⁹, A.M. Litke¹³⁷, C. Liu²⁸, D. Liu¹⁵¹, H. Liu⁸⁷, J.B. Liu⁸⁷,
 L. Liu⁸⁷, M. Liu^{32b}, Y. Liu^{32b}, M. Livan^{119a,119b}, S.S.A. Livermore¹¹⁸, A. Lleres⁵⁵, J. Llorente Merino⁸⁰,
 S.L. Lloyd⁷⁵, E. Lobodzinska⁴¹, P. Loch⁶, W.S. Lockman¹³⁷, T. Loddenkoetter²⁰, F.K. Loebinger⁸²,
 A. Loginov¹⁷⁶, C.W. Loh¹⁶⁸, T. Lohse¹⁵, K. Lohwasser⁴⁸, M. Lokajicek¹²⁵, V.P. Lombardo⁴, R.E. Long⁷¹,
 L. Lopes^{124a}, D. Lopez Mateos⁵⁷, J. Lorenz⁹⁸, N. Lorenzo Martinez¹¹⁵, M. Losada¹⁶², P. Loscutoff¹⁴,
 F. Lo Sterzo^{132a,132b}, X. Lou⁴⁰, A. Lounis¹¹⁵, K.F. Loureiro¹⁶², J. Love²¹, P.A. Love⁷¹, A.J. Lowe^{143,e},
 F. Lu^{32a}, H.J. Lubatti¹³⁸, C. Luci^{132a,132b}, A. Lucotte⁵⁵, A. Ludwig⁴³, D. Ludwig⁴¹, I. Ludwig⁴⁸,
 F. Luehring⁶⁰, W. Lukas⁶¹, L. Luminari^{132a}, E. Lund¹¹⁷, B. Lund-Jensen¹⁴⁷, B. Lundberg⁷⁹,
 J. Lundberg^{146a,146b}, O. Lundberg^{146a,146b}, J. Lundquist³⁵, M. Lungwitz⁸¹, D. Lynn²⁴, E. Lytken⁷⁹,
 H. Ma²⁴, L.L. Ma¹⁷³, G. Maccarrone⁴⁷, A. Macchiolo⁹⁹, B. Maček⁷⁴, J. Machado Miguens^{124a},
 R. Mackeprang³⁵, R.J. Madaras¹⁴, W.F. Mader⁴³, R. Maenner^{58c}, T. Maeno²⁴, P. Mättig¹⁷⁵, S. Mättig⁴¹,
 L. Magnoni²⁹, E. Magradze⁵⁴, K. Mahboubi⁴⁸, S. Mahmoud⁷³, C. Maiani¹³⁶, C. Maidantchik^{23a},
 A. Maio^{124a,b}, S. Majewski²⁴, Y. Makida⁶⁵, N. Makovec¹¹⁵, P. Mal¹³⁶, B. Malaescu²⁹, Pa. Malecki³⁸,
 P. Malecki³⁸, V.P. Maleev¹²¹, F. Malek⁵⁵, U. Mallik⁶², D. Malon⁵, C. Malone¹⁴³, S. Maltezos⁹,
 V. Malyshev¹⁰⁷, S. Malyukov²⁹, J. Mamuzic^{12b}, L. Mandelli^{89a}, I. Mandić⁷⁴, R. Mandrysch¹⁵,
 J. Maneira^{124a}, L. Manhaes de Andrade Filho^{23a}, A. Mann⁵⁴, P.M. Manning¹³⁷,
 A. Manousakis-Katsikakis⁸, B. Mansoulie¹³⁶, A. Mapelli²⁹, L. Mapelli²⁹, L. March⁸⁰, J.F. Marchand²⁸,
 F. Marchese^{133a,133b}, G. Marchiori⁷⁸, M. Marcisovsky¹²⁵, C.P. Marino¹⁶⁹, F. Marroquim^{23a}, Z. Marshall²⁹,
 L.F. Marti¹⁶, S. Marti-Garcia¹⁶⁷, B. Martin²⁹, B. Martin⁸⁸, T.A. Martin¹⁷, V.J. Martin⁴⁵,
 B. Martin dit Latour⁴⁹, S. Martin-Haugh¹⁴⁹, M. Martinez¹¹, V. Martinez Outschoorn⁵⁷,
 A.C. Martyniuk¹⁶⁹, M. Marx⁸², F. Marzano^{132a}, A. Marzin¹¹¹, L. Masetti⁸¹, T. Mashimo¹⁵⁵,
 R. Mashinistov⁹⁴, J. Masik⁸², A.L. Maslennikov¹⁰⁷, I. Massa^{19a,19b}, N. Massol⁴, A. Mastroberardino^{36a,36b},
 T. Masubuchi¹⁵⁵, P. Matricon¹¹⁵, H. Matsunaga¹⁵⁵, T. Matsushita⁶⁶, C. Mattraversi^{118,c}, J. Maurer⁸³,
 S.J. Maxfield⁷³, A. Mayne¹³⁹, R. Mazini¹⁵¹, M. Mazur²⁰, L. Mazzaferro^{133a,133b}, S.P. Mc Kee⁸⁷,
 A. McCarn¹⁶⁵, R.L. McCarthy¹⁴⁸, T.G. McCarthy²⁸, N.A. McCubbin¹²⁹, J.A. McFayden¹³⁹,
 G. Mchedlize^{51b}, T. McLaughlan¹⁷, S.J. McMahon¹²⁹, R.A. McPherson^{169,j}, A. Meade⁸⁴, J. Mechnich¹⁰⁵,
 M. Mechtel¹⁷⁵, M. Medinnis⁴¹, R. Meera-Lebbai¹¹¹, T. Meguro¹¹⁶, S. Mehlhase³⁵, A. Mehta⁷³,
 K. Meier^{58a}, B. Meirose⁷⁹, C. Melachrinou³⁰, B.R. Mellado Garcia¹⁷³, F. Meloni^{89a,89b},
 L. Mendoza Navas¹⁶², Z. Meng^{151,s}, A. Mengarelli^{19a,19b}, S. Menke⁹⁹, E. Meoni¹⁶¹, K.M. Mercurio⁵⁷,
 P. Mermod⁴⁹, L. Merola^{102a,102b}, C. Meroni^{89a}, F.S. Merritt³⁰, H. Merritt¹⁰⁹, A. Messina^{29,w},
 J. Metcalfe¹⁰³, A.S. Mete¹⁶³, C. Meyer⁸¹, C. Meyer³⁰, J-P. Meyer¹³⁶, J. Meyer¹⁷⁴, J. Meyer⁵⁴,
 T.C. Meyer²⁹, J. Miao^{32d}, S. Michal²⁹, R.P. Middleton¹²⁹, S. Migas⁷³, L. Mijović⁴¹, G. Mikenberg¹⁷²,
 M. Mikestikova¹²⁵, M. Mikuz⁷⁴, D.W. Miller³⁰, W.J. Mills¹⁶⁸, C. Mills⁵⁷, A. Milov¹⁷²,
 D.A. Milstead^{146a,146b}, D. Milstein¹⁷², A.A. Minaenko¹²⁸, M. Miñano Moya¹⁶⁷, I.A. Minashvili⁶⁴,
 A.I. Mincer¹⁰⁸, B. Mindur³⁷, M. Mineev⁶⁴, Y. Ming¹⁷³, L.M. Mir¹¹, J. Mitrevski¹³⁷, V.A. Mitsou¹⁶⁷,
 S. Mitsui⁶⁵, P.S. Miyagawa¹³⁹, J.U. Mjörnmark⁷⁹, T. Moa^{146a,146b}, V. Moeller²⁷, K. Mönig⁴¹, N. Möser²⁰,
 S. Mohapatra¹⁴⁸, R. Moles-Valls¹⁶⁷, J. Monk⁷⁷, E. Monnier⁸³, J. Montejo Berlingen¹¹, F. Monticelli⁷⁰,
 S. Monzani^{19a,19b}, R.W. Moore², C. Mora Herrera⁴⁹, A. Moraes⁵³, N. Morange¹³⁶, J. Morel⁵⁴,
 G. Morello^{36a,36b}, D. Moreno⁸¹, M. Moreno Llácer¹⁶⁷, P. Morettini^{50a}, M. Morgenstern⁴³, M. Morii⁵⁷,
 A.K. Morley²⁹, G. Mornacchi²⁹, J.D. Morris⁷⁵, L. Morvaj¹⁰¹, H.G. Moser⁹⁹, M. Mosidze^{51b}, J. Moss¹⁰⁹,
 R. Mount¹⁴³, E. Mountricha^{9,x}, E.J.W. Moyse⁸⁴, F. Mueller^{58a}, J. Mueller¹²³, K. Mueller²⁰,
 T.A. Müller⁹⁸, T. Mueller⁸¹, D. Muenstermann²⁹, Y. Munwes¹⁵³, W.J. Murray¹²⁹, I. Mussche¹⁰⁵,
 E. Musto^{102a,102b}, A.G. Myagkov¹²⁸, M. Myska¹²⁵, J. Nadal¹¹, K. Nagai¹⁶⁰, K. Nagano⁶⁵, A. Nagarkar¹⁰⁹,
 Y. Nagasaka⁵⁹, M. Nagel⁹⁹, A.M. Nairz²⁹, Y. Nakahama²⁹, K. Nakamura¹⁵⁵, T. Nakamura¹⁵⁵,

I. Nakano¹¹⁰, G. Nanava²⁰, A. Napier¹⁶¹, R. Narayan^{58b}, M. Nash^{77,c}, T. Nattermann²⁰, T. Naumann⁴¹,
 G. Navarro¹⁶², H.A. Neal⁸⁷, P.Yu. Nechaeva⁹⁴, T.J. Neep⁸², A. Negri^{119a,119b}, G. Negri²⁹,
 S. Nektarijevic⁴⁹, A. Nelson¹⁶³, T.K. Nelson¹⁴³, S. Nemecek¹²⁵, P. Nemethy¹⁰⁸, A.A. Nepomuceno^{23a},
 M. Nessi^{29,y}, M.S. Neubauer¹⁶⁵, A. Neusiedl⁸¹, R.M. Neves¹⁰⁸, P. Nevski²⁴, P.R. Newman¹⁷,
 V. Nguyen Thi Hong¹³⁶, R.B. Nickerson¹¹⁸, R. Nicolaidou¹³⁶, F. Niedercorn¹¹⁵, J. Nielsen¹³⁷,
 N. Nikiforou³⁴, A. Nikiforov¹⁵, V. Nikolaenko¹²⁸, I. Nikolic-Audit⁷⁸, K. Nikolics⁴⁹, K. Nikolopoulos²⁴,
 P. Nilsson⁷, Y. Ninomiya¹⁵⁵, A. Nisati^{132a}, R. Nisius⁹⁹, T. Nobe¹⁵⁷, L. Nodulman⁵, M. Nomachi¹¹⁶,
 I. Nomidis¹⁵⁴, M. Nordberg²⁹, J. Novakova¹²⁶, M. Nozaki⁶⁵, L. Nozka¹¹³, I.M. Nugent^{159a},
 A.-E. Nuncio-Quiroz²⁰, G. Nunes Hanninger⁸⁶, T. Nunnemann⁹⁸, E. Nurse⁷⁷, B.J. O'Brien⁴⁵,
 D.C. O'Neil¹⁴², V. O'Shea⁵³, L.B. Oakes⁹⁸, F.G. Oakham^{28,d}, H. Oberlack⁹⁹, J. Ocariz⁷⁸, A. Ochi⁶⁶,
 S. Oda⁶⁹, S. Odaka⁶⁵, J. Odier⁸³, H. Ogren⁶⁰, A. Oh⁸², S.H. Oh⁴⁴, C.C. Ohm^{146a,146b}, T. Ohshima¹⁰¹,
 H. Okawa¹⁶³, Y. Okumura¹⁰¹, T. Okuyama¹⁵⁵, A. Olariu^{25a}, S.A. Olivares Pino^{31a}, M. Oliveira^{124a,h},
 D. Oliveira Damazio²⁴, E. Oliver Garcia¹⁶⁷, D. Olivito¹²⁰, A. Olszewski³⁸, J. Olszowska³⁸, A. Onofre^{124a,z},
 P.U.E. Onyisi³⁰, M.J. Oreglia³⁰, Y. Oren¹⁵³, D. Orestano^{134a,134b}, N. Orlando^{72a,72b}, I. Orlov¹⁰⁷,
 C. Oropeza Barrera⁵³, R.S. Orr¹⁵⁸, B. Osculati^{50a,50b}, R. Ospanov¹²⁰, C. Osuna¹¹, G. Otero y Garzon²⁶,
 J.P. Ottersbach¹⁰⁵, M. Ouchrif^{135d}, E.A. Ouellette¹⁶⁹, F. Ould-Saada¹¹⁷, A. Ouraou¹³⁶, Q. Ouyang^{32a},
 A. Ovcharova¹⁴, M. Owen⁸², S. Owen¹³⁹, V.E. Ozcan^{18a}, N. Ozturk⁷, A. Pacheco Pages¹¹,
 C. Padilla Aranda¹¹, S. Pagan Griso¹⁴, E. Paganis¹³⁹, F. Paige²⁴, P. Pais⁸⁴, K. Pajchel¹¹⁷,
 G. Palacino^{159b}, C.P. Paleari⁶, S. Palestini²⁹, D. Pallin³³, A. Palma^{124a}, J.D. Palmer¹⁷, Y.B. Pan¹⁷³,
 E. Panagiotopoulou⁹, P. Pani¹⁰⁵, N. Panikashvili⁸⁷, S. Panitkin²⁴, D. Pantea^{25a}, A. Papadelis^{146a},
 Th.D. Papadopoulou⁹, A. Paramonov⁵, D. Paredes Hernandez³³, W. Park^{24,aa}, M.A. Parker²⁷,
 F. Parodi^{50a,50b}, J.A. Parsons³⁴, U. Parzefall⁴⁸, S. Pashapour⁵⁴, E. Pasqualucci^{132a}, S. Passaggio^{50a},
 Fr. Pastore⁷⁶, G. Pásztor^{49,ab}, S. Pataraiia¹⁷⁵, N. Patel¹⁵⁰, J.R. Pater⁸², S. Patricelli^{102a,102b}, T. Pauly²⁹,
 M. Pecsý^{144a}, M.I. Pedraza Morales¹⁷³, S.V. Peleganchuk¹⁰⁷, D. Pelikan¹⁶⁶, H. Peng^{32b}, B. Penning³⁰,
 A. Penson³⁴, J. Penwell⁶⁰, M. Perantoni^{23a}, K. Perez^{34,ac}, T. Perez Cavalcanti⁴¹, E. Perez Codina^{159a},
 M.T. Pérez García-Estañ¹⁶⁷, L. Perini^{89a,89b}, H. Pernegger²⁹, S. Persebe^{3a}, V.D. Peshekhonov⁶⁴,
 K. Peters²⁹, B.A. Petersen²⁹, T.C. Petersen³⁵, E. Petit⁴, A. Petridis¹⁵⁴, C. Petridou¹⁵⁴, E. Petrolo^{132a},
 F. Petrucci^{134a,134b}, D. Petschull⁴¹, M. Petteni¹⁴², R. Pezoa^{31b}, A. Phan⁸⁶, P.W. Phillips¹²⁹,
 G. Piacquadio²⁹, A. Picazio⁴⁹, E. Piccaro⁷⁵, M. Piccinini^{19a,19b}, S.M. Piec⁴¹, R. Piegaia²⁶,
 D.T. Pignotti¹⁰⁹, J.E. Pilcher³⁰, A.D. Pilkington⁸², J. Pina^{124a,b}, M. Pinamonti^{164a,164c}, A. Pinder¹¹⁸,
 J.L. Pinfold², B. Pinto^{124a}, C. Pizio^{89a,89b}, M. Plamondon¹⁶⁹, M.-A. Pleier²⁴, E. Plotnikova⁶⁴,
 A. Poblaguev²⁴, S. Poddar^{58a}, F. Podlyski³³, L. Poggioli¹¹⁵, T. Poghosyan²⁰, M. Pohl⁴⁹, G. Polesello^{119a},
 A. Policicchio^{36a,36b}, A. Polini^{19a}, J. Poll⁷⁵, V. Polychronakos²⁴, D. Pomeroy²², K. Pommès²⁹,
 L. Pontecorvo^{132a}, B.G. Pope⁸⁸, G.A. Popeneciu^{25a}, D.S. Popovic^{12a}, A. Poppleton²⁹, X. Portell Bueso²⁹,
 G.E. Pospelov⁹⁹, S. Pospisil¹²⁷, I.N. Potrap⁹⁹, C.J. Potter¹⁴⁹, C.T. Potter¹¹⁴, G. Poulard²⁹, J. Poveda⁶⁰,
 V. Pozdnyakov⁶⁴, R. Prabhu⁷⁷, P. Pralavorio⁸³, A. Pranko¹⁴, S. Prasad²⁹, R. Pravahan²⁴, S. Prell⁶³,
 D. Price⁶⁰, J. Price⁷³, L.E. Price⁵, D. Prieur¹²³, M. Primavera^{72a}, K. Prokofiev¹⁰⁸, F. Prokoshin^{31b},
 S. Protopopescu²⁴, J. Proudfoot⁵, X. Prudent⁴³, M. Przybycien³⁷, H. Przysiezniak⁴, S. Psoroulas²⁰,
 E. Ptacek¹¹⁴, E. Pueschel⁸⁴, J. Purdham⁸⁷, M. Purohit^{24,aa}, P. Puze¹¹⁵, Y. Pylypchenko⁶², J. Qian⁸⁷,
 A. Quadt⁵⁴, D.R. Quarrie¹⁴, W.B. Quayle¹⁷³, F. Quinonez^{31a}, M. Raas¹⁰⁴, V. Radescu⁴¹, P. Radloff¹¹⁴,
 T. Rador^{18a}, F. Ragusa^{89a,89b}, G. Rahal¹⁷⁸, S. Rajagopalan²⁴, M. Rammensee⁴⁸, M. Rammes¹⁴¹,
 A.S. Randle-Conde³⁹, K. Randrianarivony²⁸, F. Rauscher⁹⁸, T.C. Rave⁴⁸, M. Raymond²⁹, A.L. Read¹¹⁷,
 D.M. Rebuffi^{119a,119b}, A. Redelbach¹⁷⁴, G. Redlinger²⁴, R. Reece¹²⁰, K. Reeves⁴⁰, A. Reinsch¹¹⁴,
 I. Reisinger⁴², C. Rembser²⁹, Z.L. Ren¹⁵¹, A. Renaud¹¹⁵, M. Rescigno^{132a}, S. Resconi^{89a}, B. Resende¹³⁶,
 P. Reznicek⁹⁸, R. Rezvani¹⁵⁸, R. Richter⁹⁹, E. Richter-Was^{4,ad}, M. Ridel⁷⁸, M. Rijssenbeek¹⁴⁸,
 A. Rimoldi^{119a,119b}, L. Rinaldi^{19a}, R.R. Rios³⁹, I. Riu¹¹, F. Rizatdinova¹¹², E. Rizvi⁷⁵, S.H. Robertson^{85,j},
 A. Robichaud-Veronneau¹¹⁸, D. Robinson²⁷, J.E.M. Robinson⁷⁷, A. Robson⁵³, J.G. Rocha de Lima¹⁰⁶,
 C. Roda^{122a,122b}, D. Roda Dos Santos²⁹, A. Roe⁵⁴, S. Roe²⁹, O. Røhne¹¹⁷, A. Romaniouk⁹⁶,
 M. Romano^{19a,19b}, G. Romeo²⁶, E. Romero Adam¹⁶⁷, L. Roos⁷⁸, E. Ros¹⁶⁷, S. Rosati^{132a}, K. Rosbach⁴⁹,
 A. Rose¹⁴⁹, M. Rose⁷⁶, G.A. Rosenbaum¹⁵⁸, P.L. Rosendahl¹³, O. Rosenthal¹⁴¹, V. Rossetti¹¹,
 E. Rossi^{132a,132b}, L.P. Rossi^{50a}, M. Rotaru^{25a}, I. Roth¹⁷², J. Rothberg¹³⁸, D. Rousseau¹¹⁵, C.R. Royon¹³⁶,
 A. Rozanov⁸³, Y. Rozen¹⁵², X. Ruan^{32a,ae}, F. Rubbo¹¹, I. Rubinskiy⁴¹, N. Ruckstuhl¹⁰⁵, V.I. Rud⁹⁷,

C. Rudolph⁴³, G. Rudolph⁶¹, F. Rühr⁶, A. Ruiz-Martinez⁶³, Z. Rurikova⁴⁸, N.A. Rusakovich⁶⁴,
 J.P. Rutherford⁶, C. Ruwiedel¹⁴, P. Ruzicka¹²⁵, Y.F. Ryabov¹²¹, M. Rybar¹²⁶, G. Rybkin¹¹⁵,
 N.C. Ryder¹¹⁸, A.F. Saavedra¹⁵⁰, I. Sadeh¹⁵³, H.F.-W. Sadrozinski¹³⁷, R. Sadykov⁶⁴, F. Safai Tehrani^{132a},
 H. Sakamoto¹⁵⁵, G. Salamanna⁷⁵, A. Salamon^{133a}, M. Saleem¹¹¹, D. Salek²⁹, D. Salihagic⁹⁹,
 A. Salnikov¹⁴³, J. Salt¹⁶⁷, B.M. Salvachua Ferrando⁵, D. Salvatore^{36a,36b}, F. Salvatore¹⁴⁹, A. Salvucci¹⁰⁴,
 A. Salzburger²⁹, D. Sampsonidis¹⁵⁴, A. Sanchez^{102a,102b}, V. Sanchez Martinez¹⁶⁷, H. Sandaker¹³,
 H.G. Sander⁸¹, M.P. Sanders⁹⁸, M. Sandhoff¹⁷⁵, T. Sandoval²⁷, C. Sandoval¹⁶², R. Sandstroem⁹⁹,
 D.P.C. Sankey¹²⁹, A. Sansoni⁴⁷, C. Santoni³³, R. Santonico^{133a,133b}, H. Santos^{124a}, J.G. Saraiva^{124a},
 T. Sarangi¹⁷³, E. Sarkisyan-Grinbaum⁷, G. Sartiso¹⁷⁵, O. Sasaki⁶⁵, N. Sasao⁶⁷, I. Satsounkevitch⁹⁰,
 E. Sauvan⁴, J.B. Sauvan¹¹⁵, P. Savard^{158,d}, V. Savinov¹²³, D.O. Savu²⁹, L. Sawyer^{24,l}, J. Saxon¹²⁰,
 C. Sbarra^{19a}, A. Sbrizzi^{19a,19b}, O. Scallan⁹³, D.A. Scannicchio¹⁶³, M. Scarcella¹⁵⁰, J. Schaarschmidt¹¹⁵,
 P. Schacht⁹⁹, D. Schaefer¹²⁰, U. Schäfer⁸¹, S. Schaepe²⁰, S. Schaezel^{58b}, A.C. Schaffer¹¹⁵, D. Schaile⁹⁸,
 R.D. Schamberger¹⁴⁸, A.G. Schamov¹⁰⁷, V. Scharf^{58a}, V.A. Schegelsky¹²¹, D. Scheirich⁸⁷, M. Schernau¹⁶³,
 M.I. Scherzer³⁴, C. Schiavi^{50a,50b}, J. Schieck⁹⁸, M. Schioppa^{36a,36b}, S. Schlenker²⁹, E. Schmidt⁴⁸,
 K. Schmieden²⁰, C. Schmitt⁸¹, S. Schmitt^{58b}, M. Schmitz²⁰, B. Schneider¹⁶, U. Schnoor⁴³, A. Schöning^{58b},
 M. Schott²⁹, D. Schouten^{159a}, J. Schovancova¹²⁵, M. Schram⁸⁵, C. Schroeder⁸¹, N. Schroer^{58c},
 M.J. Schultens²⁰, J. Schultes¹⁷⁵, H.-C. Schultz-Coulon^{58a}, H. Schulz¹⁵, M. Schumacher⁴⁸, B.A. Schumm¹³⁷,
 Ph. Schune¹³⁶, C. Schwanenberger⁸², A. Schwartzman¹⁴³, Ph. Schwemling⁷⁸, R. Schwienhorst⁸⁸,
 J. Schwindling¹³⁶, T. Schwindt²⁰, M. Schwoerer⁴, G. Sciolla²², W.G. Scott¹²⁹, J. Searcy¹¹⁴, G. Sedov⁴¹,
 E. Sedykh¹²¹, S.C. Seidel¹⁰³, A. Seiden¹³⁷, F. Seifert⁴³, J.M. Seixas^{23a}, G. Sekhniaidze^{102a}, S.J. Sekula³⁹,
 K.E. Selbach⁴⁵, D.M. Seliverstov¹²¹, G. Sellers⁷³, N. Semprini-Cesari^{19a,19b}, C. Serfon⁹⁸, L. Serin¹¹⁵,
 L. Serkin⁵⁴, R. Seuster⁹⁹, H. Severini¹¹¹, A. Sfyrta²⁹, E. Shabalina⁵⁴, M. Shamim¹¹⁴, L.Y. Shan^{32a},
 J.T. Shank²¹, Q.T. Shao⁸⁶, M. Shapiro¹⁴, P.B. Shatalov⁹⁵, K. Shaw^{164a,164c}, D. Sherman¹⁷⁶,
 P. Sherwood⁷⁷, S. Shimizu²⁹, M. Shimojima¹⁰⁰, T. Shin⁵⁶, M. Shiyakova⁶⁴, A. Shmeleva⁹⁴, M.J. Shochet³⁰,
 D. Short¹¹⁸, S. Shrestha⁶³, E. Shulga⁹⁶, M.A. Shupe⁶, P. Sicho¹²⁵, A. Sidoti^{132a}, F. Siegert⁴⁸,
 Dj. Sijacki^{12a}, O. Silbert¹⁷², J. Silva^{124a}, Y. Silver¹⁵³, D. Silverstein¹⁴³, S.B. Silverstein^{146a}, V. Simak¹²⁷,
 O. Simard¹³⁶, Lj. Simic^{12a}, S. Simion¹¹⁵, E. Simioni⁸¹, B. Simmons⁷⁷, R. Simoniello^{89a,89b}, M. Simonyan³⁵,
 P. Sinervo¹⁵⁸, N.B. Sinev¹¹⁴, V. Sipica¹⁴¹, G. Siragusa¹⁷⁴, A. Sircar²⁴, S.Yu. Sivoklov⁹⁷, J. Sjölin^{146a,146b},
 T.B. Sjursen¹³, L.A. Skinnari¹⁴, H.P. Skottowe⁵⁷, K. Skovpen¹⁰⁷, P. Skubic¹¹¹, M. Slater¹⁷, T. Slavicek¹²⁷,
 K. Sliwa¹⁶¹, V. Smakhtin¹⁷², B.H. Smart⁴⁵, S.Yu. Smirnov⁹⁶, Y. Smirnov⁹⁶, L.N. Smirnova⁹⁷,
 O. Smirnova⁷⁹, B.C. Smith⁵⁷, D. Smith¹⁴³, M. Smizanska⁷¹, K. Smolek¹²⁷, A.A. Snesarev⁹⁴, J. Snow¹¹¹,
 S. Snyder²⁴, R. Sobie^{169,j}, A. Soffer¹⁵³, C.A. Solans¹⁶⁷, M. Solar¹²⁷, J. Solc¹²⁷, E. Soldatov⁹⁶,
 U. Soldevila¹⁶⁷, E. Solfaroli Camillocci^{132a,132b}, A.A. Solodkov¹²⁸, O.V. Solovyanov¹²⁸, N. Soni²,
 V. Sopko¹²⁷, B. Sopko¹²⁷, M. Sosebee⁷, R. Soualah^{164a,164c}, A. Soukharev¹⁰⁷, S. Spagnolo^{72a,72b},
 F. Spanò⁷⁶, R. Spighi^{19a}, G. Spigo²⁹, R. Spiwox²⁹, M. Spusta¹²⁶, T. Spreitzer¹⁵⁸, R.D. St. Denis⁵³,
 J. Stahlman¹²⁰, R. Stamen^{58a}, E. Stanecka³⁸, R.W. Stanek⁵, C. Stanescu^{134a}, M. Stanescu-Bellu⁴¹,
 S. Stapnes¹¹⁷, E.A. Starchenko¹²⁸, J. Stark⁵⁵, P. Staroba¹²⁵, P. Starovoitov⁴¹, R. Staszewski³⁸, G. Steele⁵³,
 P. Steinbach⁴³, P. Steinberg²⁴, B. Stelzer¹⁴², H.J. Stelzer⁸⁸, O. Stelzer-Chilton^{159a}, H. Stenzel⁵²,
 S. Stern⁹⁹, G.A. Stewart²⁹, J.A. Stillings²⁰, M.C. Stockton⁸⁵, K. Stoerig⁴⁸, G. Stoicea^{25a}, S. Stonjek⁹⁹,
 P. Strachota¹²⁶, A.R. Stradling⁷, A. Straessner⁴³, J. Strandberg¹⁴⁷, S. Strandberg^{146a,146b}, A. Strandlie¹¹⁷,
 M. Strang¹⁰⁹, E. Strauss¹⁴³, M. Strauss¹¹¹, P. Strizenc^{144b}, R. Ströhmer¹⁷⁴, D.M. Strom¹¹⁴,
 R. Stroynowski³⁹, J. Strube¹²⁹, B. Stugu¹³, J. Stupak¹⁴⁸, P. Sturm¹⁷⁵, N.A. Styles⁴¹, D.A. Soh^{151,u},
 D. Su¹⁴³, HS. Subramania², A. Succurro¹¹, Y. Sugaya¹¹⁶, C. Suhr¹⁰⁶, M. Suk¹²⁶, V.V. Sulin⁹⁴,
 S. Sultansoy^{3d}, T. Sumida⁶⁷, X. Sun⁵⁵, J.E. Sundermann⁴⁸, K. Suruliz¹³⁹, G. Susinno^{36a,36b},
 M.R. Sutton¹⁴⁹, Y. Suzuki⁶⁵, Y. Suzuki⁶⁶, M. Svatos¹²⁵, S. Swedish¹⁶⁸, I. Sykora^{144a}, T. Sykora¹²⁶,
 J. Sánchez¹⁶⁷, D. Ta¹⁰⁵, K. Tackmann⁴¹, A. Taffard¹⁶³, R. Tafirout^{159a}, N. Taiblum¹⁵³, Y. Takahashi¹⁰¹,
 H. Takai²⁴, R. Takashima⁶⁸, H. Takeda⁶⁶, T. Takeshita¹⁴⁰, Y. Takubo⁶⁵, M. Talby⁸³, A. Talyshev^{107,f},
 M.C. Tamssett²⁴, J. Tanaka¹⁵⁵, R. Tanaka¹¹⁵, S. Tanaka⁶⁵, A.J. Tanasijczuk¹⁴², K. Tani⁶⁶, N. Tannoury⁸³,
 S. Tapprogge⁸¹, D. Tardif¹⁵⁸, S. Tarem¹⁵², F. Tarrade²⁸, G.F. Tartarelli^{89a}, P. Tas¹²⁶, M. Tasevsky¹²⁵,
 E. Tassi^{36a,36b}, M. Tatarkhanov¹⁴, Y. Tayalati^{135d}, C. Taylor⁷⁷, F.E. Taylor⁹², G.N. Taylor⁸⁶,
 W. Taylor^{159b}, M. Teinturier¹¹⁵, M. Teixeira Dias Castanheira⁷⁵, P. Teixeira-Dias⁷⁶, K.K. Temming⁴⁸,
 H. Ten Kate²⁹, P.K. Teng¹⁵¹, S. Terada⁶⁵, K. Terashi¹⁵⁵, J. Terron⁸⁰, M. Testa⁴⁷, R.J. Teuscher^{158,j},

J. Therhaag²⁰, T. Theveneaux-Pelzer⁷⁸, S. Thoma⁴⁸, J.P. Thomas¹⁷, E.N. Thompson³⁴, P.D. Thompson¹⁷,
 P.D. Thompson¹⁵⁸, A.S. Thompson⁵³, L.A. Thomsen³⁵, E. Thomson¹²⁰, M. Thomson²⁷, R.P. Thun⁸⁷,
 F. Tian³⁴, M.J. Tibbetts¹⁴, T. Tic¹²⁵, V.O. Tikhomirov⁹⁴, Y.A. Tikhonov^{107,f}, S. Timoshenko⁹⁶,
 P. Tipton¹⁷⁶, F.J. Tique Aires Viegas²⁹, S. Tisserant⁸³, T. Todorov⁴, S. Todorova-Nova¹⁶¹,
 B. Toggerson¹⁶³, J. Tojo⁶⁹, S. Tokár^{144a}, K. Tokushuku⁶⁵, K. Tollefson⁸⁸, M. Tomoto¹⁰¹, L. Tompkins³⁰,
 K. Toms¹⁰³, A. Tonoyan¹³, C. Topfel¹⁶, I. Torchiani²⁹, E. Torrence¹¹⁴, H. Torres⁷⁸, E. Torró Pastor¹⁶⁷,
 J. Toth^{83,ab}, F. Touchard⁸³, D.R. Tovey¹³⁹, T. Trefzger¹⁷⁴, L. Tremblet²⁹, A. Tricoli²⁹, I.M. Trigger^{159a},
 S. Trincaz-Duvoid⁷⁸, M.F. Tripiana⁷⁰, W. Trischuk¹⁵⁸, B. Trocmé⁵⁵, C. Troncon^{89a},
 M. Trottier-McDonald¹⁴², M. Trzebinski³⁸, A. Trzupiek³⁸, C. Tsarouchas²⁹, J.C-L. Tseng¹¹⁸,
 M. Tsiakiris¹⁰⁵, P.V. Tsiareshka⁹⁰, D. Tsionou^{4,af}, G. Tsipolitis⁹, V. Tsiskaridze⁴⁸, E.G. Tskhadadze^{51a},
 I.I. Tsukerman⁹⁵, V. Tsulaia¹⁴, J.-W. Tsung²⁰, S. Tsuno⁶⁵, D. Tsybychev¹⁴⁸, A. Tua¹³⁹, A. Tudorache^{25a},
 V. Tudorache^{25a}, J.M. Tuggle³⁰, D. Turecek¹²⁷, I. Turk Cakir^{3e}, E. Turley¹⁰⁵, R. Turra^{89a,89b}, P.M. Tuts³⁴,
 A. Tykhonov⁷⁴, M. Tylmad^{146a,146b}, K. Uchida²⁰, I. Ueda¹⁵⁵, R. Ueno²⁸, M. Ugland¹³, M. Uhlenbrock²⁰,
 M. Uhrmacher⁵⁴, F. Ukegawa¹⁶⁰, G. Unal²⁹, A. Undrus²⁴, G. Unel¹⁶³, Y. Unno⁶⁵, D. Urbaniec³⁴, G. Usai⁷,
 M. Uslenghi^{119a,119b}, L. Vacavant⁸³, V. Vacek¹²⁷, B. Vachon⁸⁵, S. Valentinetti^{19a,19b}, S. Valkar¹²⁶,
 E. Valladolid Gallego¹⁶⁷, S. Vallecorsa¹⁵², J.A. Valls Ferrer¹⁶⁷, H. van der Graaf¹⁰⁵, R. Van Der Leeuw¹⁰⁵,
 E. van der Poel¹⁰⁵, D. van der Ster²⁹, N. van Eldik⁸⁴, P. van Gemmeren⁵, I. van Vulpen¹⁰⁵, M. Vanadia⁹⁹,
 W. Vandelli²⁹, A. Vaniachine⁵, P. Vankov⁴¹, F. Vannucci⁷⁸, R. Vari^{132a}, T. Varol⁸⁴, D. Varouchas¹⁴,
 A. Vartapetian⁷, K.E. Varvell¹⁵⁰, V.I. Vassilakopoulos⁵⁶, F. Vazeille³³, T. Vazquez Schroeder⁵⁴,
 F. Veloso^{124a}, S. Veneziano^{132a}, A. Ventura^{72a,72b}, D. Ventura⁸⁴, M. Venturi⁴⁸, N. Venturi¹⁵⁸,
 V. Vercesi^{119a}, M. Verducci¹³⁸, W. Verkerke¹⁰⁵, J.C. Vermeulen¹⁰⁵, A. Vest⁴³, M.C. Vetterli^{142,d},
 I. Vichou¹⁶⁵, T. Vickey^{145b,ag}, O.E. Vickey Boeriu^{145b}, G.H.A. Viehhauser¹¹⁸, S. Viel¹⁶⁸, M. Villa^{19a,19b},
 M. Villaplana Perez¹⁶⁷, E. Vilucchi⁴⁷, M.G. Vinciter²⁸, E. Vinek²⁹, V.B. Vinogradov⁶⁴, J. Virzi¹⁴,
 O. Vitells¹⁷², M. Viti⁴¹, I. Vivarelli⁴⁸, F. Vives Vaque², S. Vlachos⁹, D. Vladoiu⁹⁸, M. Vlasak¹²⁷,
 A. Vogel²⁰, P. Vokac¹²⁷, G. Volpi⁴⁷, M. Volpi⁸⁶, H. von der Schmitt⁹⁹, J. von Loeben⁹⁹,
 H. von Radziewski⁴⁸, E. von Toerne²⁰, V. Vorobel¹²⁶, V. Vorwerk¹¹, M. Vos¹⁶⁷, R. Voss²⁹, T.T. Voss¹⁷⁵,
 J.H. Vossebeld⁷³, N. Vranjes¹³⁶, M. Vranjes Milosavljevic¹⁰⁵, V. Vrba¹²⁵, M. Vreeswijk¹⁰⁵, T. Vu Anh⁴⁸,
 R. Vuillermet²⁹, I. Vukotic¹¹⁵, W. Wagner¹⁷⁵, P. Wagner¹²⁰, S. Wahrenmund⁴³, J. Wakabayashi¹⁰¹,
 S. Walch⁸⁷, J. Walder⁷¹, R. Walker⁹⁸, W. Walkowiak¹⁴¹, R. Wall¹⁷⁶, P. Waller⁷³, C. Wang⁴⁴, H. Wang¹⁷³,
 H. Wang^{32b,ah}, J. Wang¹⁵¹, J. Wang⁵⁵, R. Wang¹⁰³, S.M. Wang¹⁵¹, T. Wang²⁰, A. Warburton⁸⁵,
 C.P. Ward²⁷, M. Warsinsky⁴⁸, A. Washbrook⁴⁵, C. Wasicki⁴¹, P.M. Watkins¹⁷, A.T. Watson¹⁷,
 I.J. Watson¹⁵⁰, M.F. Watson¹⁷, G. Watts¹³⁸, S. Watts⁸², A.T. Waugh¹⁵⁰, B.M. Waugh⁷⁷, M.S. Weber¹⁶,
 P. Weber⁵⁴, A.R. Weidberg¹¹⁸, P. Weigell⁹⁹, J. Weingarten⁵⁴, C. Weiser⁴⁸, P.S. Wells²⁹, T. Wenaus²⁴,
 D. Wendland¹⁵, Z. Weng^{151,u}, T. Wengler²⁹, S. Wenig²⁹, N. Wermes²⁰, M. Werner⁴⁸, P. Werner²⁹,
 M. Werth¹⁶³, M. Wessels^{58a}, J. Wetter¹⁶¹, C. Weydert⁵⁵, K. Whalen²⁸, A. White⁷, M.J. White⁸⁶,
 S.R. Whitehead¹¹⁸, D. Whiteson¹⁶³, D. Whittington⁶⁰, F. Wicek¹¹⁵, D. Wicke¹⁷⁵, F.J. Wickens¹²⁹,
 W. Wiedenmann¹⁷³, M. Wielers¹²⁹, P. Wienemann²⁰, C. Wiglesworth⁷⁵, L.A.M. Wiik-Fuchs⁴⁸,
 P.A. Wijeratne⁷⁷, A. Wildauer¹⁶⁷, M.A. Wildt^{41,q}, H.G. Wilkens²⁹, J.Z. Will⁹⁸, E. Williams³⁴,
 H.H. Williams¹²⁰, S. Willocq⁸⁴, J.A. Wilson¹⁷, M.G. Wilson¹⁴³, A. Wilson⁸⁷, I. Wingerter-Seez⁴,
 S. Winkelmann⁴⁸, F. Winklmeier²⁹, M. Wittgen¹⁴³, M.W. Wolter³⁸, H. Wolters^{124a,h}, W.C. Wong⁴⁰,
 G. Wooden⁸⁷, B.K. Wosiek³⁸, J. Wotschack²⁹, M.J. Woudstra⁸⁴, K.W. Wozniak³⁸, K. Wraight⁵³,
 M. Wright⁵³, B. Wrona⁷³, S.L. Wu¹⁷³, X. Wu⁴⁹, Y. Wu^{32b,ai}, E. Wulf³⁴, B.M. Wynne⁴⁵, S. Xella³⁵,
 M. Xiao¹³⁶, S. Xie⁴⁸, C. Xu^{32b,x}, D. Xu¹³⁹, B. Yabsley¹⁵⁰, S. Yacoub^{145b}, M. Yamada⁶⁵, H. Yamaguchi¹⁵⁵,
 A. Yamamoto⁶⁵, K. Yamamoto⁶³, S. Yamamoto¹⁵⁵, T. Yamamura¹⁵⁵, T. Yamanaka¹⁵⁵, J. Yamaoka⁴⁴,
 T. Yamazaki¹⁵⁵, Y. Yamazaki⁶⁶, Z. Yan²¹, H. Yang⁸⁷, U.K. Yang⁸², Y. Yang⁶⁰, Z. Yang^{146a,146b},
 S. Yanush⁹¹, L. Yao^{32a}, Y. Yao¹⁴, Y. Yasu⁶⁵, G.V. Ybeles Smit¹³⁰, J. Ye³⁹, S. Ye²⁴, M. Yilmaz^{3c},
 R. Yoosoofmiya¹²³, K. Yorita¹⁷¹, R. Yoshida⁵, C. Young¹⁴³, C.J. Young¹¹⁸, S. Youssef²¹, J. Yu⁷, J. Yu¹¹²,
 L. Yuan⁶⁶, A. Yurkewicz¹⁰⁶, B. Zabinski³⁸, R. Zaidan⁶², A.M. Zaitsev¹²⁸, Z. Zajacova²⁹, L. Zanello^{132a,132b},
 A. Zaytsev¹⁰⁷, C. Zeitnitz¹⁷⁵, M. Zeman¹²⁵, A. Zemla³⁸, C. Zendler²⁰, O. Zenin¹²⁸, T. Ženiš^{144a},
 Z. Zinonos^{122a,122b}, S. Zenz¹⁴, D. Zerwas¹¹⁵, G. Zevi della Porta⁵⁷, Z. Zhan^{32d}, D. Zhang^{32b,ah},
 H. Zhang⁸⁸, J. Zhang⁵, X. Zhang^{32d}, Z. Zhang¹¹⁵, L. Zhao¹⁰⁸, T. Zhao¹³⁸, Z. Zhao^{32b}, A. Zhemchugov⁶⁴,
 J. Zhong¹¹⁸, B. Zhou⁸⁷, N. Zhou¹⁶³, C.G. Zhu^{32d}, H. Zhu⁴¹, J. Zhu⁸⁷, Y. Zhu^{32b}, X. Zhuang⁹⁸,

V. Zhuravlov⁹⁹, D. Zieminska⁶⁰, N.I. Zimin⁶⁴, R. Zimmermann²⁰, S. Zimmermann²⁰, S. Zimmermann⁴⁸, M. Ziolkowski¹⁴¹, G. Zobernig¹⁷³, A. Zoccoli^{19a,19b}, M. zur Nedden¹⁵, V. Zutshi¹⁰⁶, L. Zwalinski²⁹.

¹ University at Albany, Albany NY, United States of America

² Department of Physics, University of Alberta, Edmonton AB, Canada

³ ^(a)Department of Physics, Ankara University, Ankara; ^(b)Department of Physics, Dumlupinar University, Kutahya; ^(c)Department of Physics, Gazi University, Ankara; ^(d)Division of Physics, TOBB University of Economics and Technology, Ankara; ^(e)Turkish Atomic Energy Authority, Ankara, Turkey

⁴ LAPP, CNRS/IN2P3 and Université de Savoie, Annecy-le-Vieux, France

⁵ High Energy Physics Division, Argonne National Laboratory, Argonne IL, United States of America

⁶ Department of Physics, University of Arizona, Tucson AZ, United States of America

⁷ Department of Physics, The University of Texas at Arlington, Arlington TX, United States of America

⁸ Physics Department, University of Athens, Athens, Greece

⁹ Physics Department, National Technical University of Athens, Zografou, Greece

¹⁰ Institute of Physics, Azerbaijan Academy of Sciences, Baku, Azerbaijan

¹¹ Institut de Física d'Altes Energies and Departament de Física de la Universitat Autònoma de Barcelona and ICREA, Barcelona, Spain

¹² ^(a)Institute of Physics, University of Belgrade, Belgrade; ^(b)Vinca Institute of Nuclear Sciences, University of Belgrade, Belgrade, Serbia

¹³ Department for Physics and Technology, University of Bergen, Bergen, Norway

¹⁴ Physics Division, Lawrence Berkeley National Laboratory and University of California, Berkeley CA, United States of America

¹⁵ Department of Physics, Humboldt University, Berlin, Germany

¹⁶ Albert Einstein Center for Fundamental Physics and Laboratory for High Energy Physics, University of Bern, Bern, Switzerland

¹⁷ School of Physics and Astronomy, University of Birmingham, Birmingham, United Kingdom

¹⁸ ^(a)Department of Physics, Bogazici University, Istanbul; ^(b)Division of Physics, Dogus University, Istanbul; ^(c)Department of Physics Engineering, Gaziantep University, Gaziantep; ^(d)Department of Physics, Istanbul Technical University, Istanbul, Turkey

¹⁹ ^(a)INFN Sezione di Bologna; ^(b)Dipartimento di Fisica, Università di Bologna, Bologna, Italy

²⁰ Physikalisches Institut, University of Bonn, Bonn, Germany

²¹ Department of Physics, Boston University, Boston MA, United States of America

²² Department of Physics, Brandeis University, Waltham MA, United States of America

²³ ^(a)Universidade Federal do Rio De Janeiro COPPE/EE/IF, Rio de Janeiro; ^(b)Federal University of Juiz de Fora (UFJF), Juiz de Fora; ^(c)Federal University of Sao Joao del Rei (UFSJ), Sao Joao del Rei; ^(d)Instituto de Fisica, Universidade de Sao Paulo, Sao Paulo, Brazil

²⁴ Physics Department, Brookhaven National Laboratory, Upton NY, United States of America

²⁵ ^(a)National Institute of Physics and Nuclear Engineering, Bucharest; ^(b)University Politehnica Bucharest, Bucharest; ^(c)West University in Timisoara, Timisoara, Romania

²⁶ Departamento de Física, Universidad de Buenos Aires, Buenos Aires, Argentina

²⁷ Cavendish Laboratory, University of Cambridge, Cambridge, United Kingdom

²⁸ Department of Physics, Carleton University, Ottawa ON, Canada

²⁹ CERN, Geneva, Switzerland

³⁰ Enrico Fermi Institute, University of Chicago, Chicago IL, United States of America

³¹ ^(a)Departamento de Física, Pontificia Universidad Católica de Chile, Santiago; ^(b)Departamento de Física, Universidad Técnica Federico Santa María, Valparaíso, Chile

³² ^(a)Institute of High Energy Physics, Chinese Academy of Sciences, Beijing; ^(b)Department of Modern Physics, University of Science and Technology of China, Anhui; ^(c)Department of Physics, Nanjing University, Jiangsu; ^(d)School of Physics, Shandong University, Shandong, China

³³ Laboratoire de Physique Corpusculaire, Clermont Université and Université Blaise Pascal and CNRS/IN2P3, Aubiere Cedex, France

³⁴ Nevis Laboratory, Columbia University, Irvington NY, United States of America

³⁵ Niels Bohr Institute, University of Copenhagen, Kobenhavn, Denmark
³⁶ ^(a)INFN Gruppo Collegato di Cosenza; ^(b)Dipartimento di Fisica, Università della Calabria, Arcavata di Rende, Italy
³⁷ AGH University of Science and Technology, Faculty of Physics and Applied Computer Science, Krakow, Poland
³⁸ The Henryk Niewodniczanski Institute of Nuclear Physics, Polish Academy of Sciences, Krakow, Poland
³⁹ Physics Department, Southern Methodist University, Dallas TX, United States of America
⁴⁰ Physics Department, University of Texas at Dallas, Richardson TX, United States of America
⁴¹ DESY, Hamburg and Zeuthen, Germany
⁴² Institut für Experimentelle Physik IV, Technische Universität Dortmund, Dortmund, Germany
⁴³ Institut für Kern- und Teilchenphysik, Technical University Dresden, Dresden, Germany
⁴⁴ Department of Physics, Duke University, Durham NC, United States of America
⁴⁵ SUPA - School of Physics and Astronomy, University of Edinburgh, Edinburgh, United Kingdom
⁴⁶ Fachhochschule Wiener Neustadt, Johannes Gutenbergstrasse 3 2700 Wiener Neustadt, Austria
⁴⁷ INFN Laboratori Nazionali di Frascati, Frascati, Italy
⁴⁸ Fakultät für Mathematik und Physik, Albert-Ludwigs-Universität, Freiburg i.Br., Germany
⁴⁹ Section de Physique, Université de Genève, Geneva, Switzerland
⁵⁰ ^(a)INFN Sezione di Genova; ^(b)Dipartimento di Fisica, Università di Genova, Genova, Italy
⁵¹ ^(a)E.Andronikashvili Institute of Physics, Tbilisi State University, Tbilisi; ^(b)High Energy Physics Institute, Tbilisi State University, Tbilisi, Georgia
⁵² II Physikalisches Institut, Justus-Liebig-Universität Giessen, Giessen, Germany
⁵³ SUPA - School of Physics and Astronomy, University of Glasgow, Glasgow, United Kingdom
⁵⁴ II Physikalisches Institut, Georg-August-Universität, Göttingen, Germany
⁵⁵ Laboratoire de Physique Subatomique et de Cosmologie, Université Joseph Fourier and CNRS/IN2P3 and Institut National Polytechnique de Grenoble, Grenoble, France
⁵⁶ Department of Physics, Hampton University, Hampton VA, United States of America
⁵⁷ Laboratory for Particle Physics and Cosmology, Harvard University, Cambridge MA, United States of America
⁵⁸ ^(a)Kirchhoff-Institut für Physik, Ruprecht-Karls-Universität Heidelberg, Heidelberg; ^(b)Physikalisches Institut, Ruprecht-Karls-Universität Heidelberg, Heidelberg; ^(c)ZITI Institut für technische Informatik, Ruprecht-Karls-Universität Heidelberg, Mannheim, Germany
⁵⁹ Faculty of Applied Information Science, Hiroshima Institute of Technology, Hiroshima, Japan
⁶⁰ Department of Physics, Indiana University, Bloomington IN, United States of America
⁶¹ Institut für Astro- und Teilchenphysik, Leopold-Franzens-Universität, Innsbruck, Austria
⁶² University of Iowa, Iowa City IA, United States of America
⁶³ Department of Physics and Astronomy, Iowa State University, Ames IA, United States of America
⁶⁴ Joint Institute for Nuclear Research, JINR Dubna, Dubna, Russia
⁶⁵ KEK, High Energy Accelerator Research Organization, Tsukuba, Japan
⁶⁶ Graduate School of Science, Kobe University, Kobe, Japan
⁶⁷ Faculty of Science, Kyoto University, Kyoto, Japan
⁶⁸ Kyoto University of Education, Kyoto, Japan
⁶⁹ Department of Physics, Kyushu University, Fukuoka, Japan
⁷⁰ Instituto de Física La Plata, Universidad Nacional de La Plata and CONICET, La Plata, Argentina
⁷¹ Physics Department, Lancaster University, Lancaster, United Kingdom
⁷² ^(a)INFN Sezione di Lecce; ^(b)Dipartimento di Matematica e Fisica, Università del Salento, Lecce, Italy
⁷³ Oliver Lodge Laboratory, University of Liverpool, Liverpool, United Kingdom
⁷⁴ Department of Physics, Jožef Stefan Institute and University of Ljubljana, Ljubljana, Slovenia
⁷⁵ School of Physics and Astronomy, Queen Mary University of London, London, United Kingdom
⁷⁶ Department of Physics, Royal Holloway University of London, Surrey, United Kingdom
⁷⁷ Department of Physics and Astronomy, University College London, London, United Kingdom
⁷⁸ Laboratoire de Physique Nucléaire et de Hautes Energies, UPMC and Université Paris-Diderot and CNRS/IN2P3, Paris, France

- 79 Fysiska institutionen, Lunds universitet, Lund, Sweden
- 80 Departamento de Fisica Teorica C-15, Universidad Autonoma de Madrid, Madrid, Spain
- 81 Institut für Physik, Universität Mainz, Mainz, Germany
- 82 School of Physics and Astronomy, University of Manchester, Manchester, United Kingdom
- 83 CPPM, Aix-Marseille Université and CNRS/IN2P3, Marseille, France
- 84 Department of Physics, University of Massachusetts, Amherst MA, United States of America
- 85 Department of Physics, McGill University, Montreal QC, Canada
- 86 School of Physics, University of Melbourne, Victoria, Australia
- 87 Department of Physics, The University of Michigan, Ann Arbor MI, United States of America
- 88 Department of Physics and Astronomy, Michigan State University, East Lansing MI, United States of America
- 89 ^(a)INFN Sezione di Milano; ^(b)Dipartimento di Fisica, Università di Milano, Milano, Italy
- 90 B.I. Stepanov Institute of Physics, National Academy of Sciences of Belarus, Minsk, Republic of Belarus
- 91 National Scientific and Educational Centre for Particle and High Energy Physics, Minsk, Republic of Belarus
- 92 Department of Physics, Massachusetts Institute of Technology, Cambridge MA, United States of America
- 93 Group of Particle Physics, University of Montreal, Montreal QC, Canada
- 94 P.N. Lebedev Institute of Physics, Academy of Sciences, Moscow, Russia
- 95 Institute for Theoretical and Experimental Physics (ITEP), Moscow, Russia
- 96 Moscow Engineering and Physics Institute (MEPhI), Moscow, Russia
- 97 Skobeltsyn Institute of Nuclear Physics, Lomonosov Moscow State University, Moscow, Russia
- 98 Fakultät für Physik, Ludwig-Maximilians-Universität München, München, Germany
- 99 Max-Planck-Institut für Physik (Werner-Heisenberg-Institut), München, Germany
- 100 Nagasaki Institute of Applied Science, Nagasaki, Japan
- 101 Graduate School of Science, Nagoya University, Nagoya, Japan
- 102 ^(a)INFN Sezione di Napoli; ^(b)Dipartimento di Scienze Fisiche, Università di Napoli, Napoli, Italy
- 103 Department of Physics and Astronomy, University of New Mexico, Albuquerque NM, United States of America
- 104 Institute for Mathematics, Astrophysics and Particle Physics, Radboud University Nijmegen/Nikhef, Nijmegen, Netherlands
- 105 Nikhef National Institute for Subatomic Physics and University of Amsterdam, Amsterdam, Netherlands
- 106 Department of Physics, Northern Illinois University, DeKalb IL, United States of America
- 107 Budker Institute of Nuclear Physics, SB RAS, Novosibirsk, Russia
- 108 Department of Physics, New York University, New York NY, United States of America
- 109 Ohio State University, Columbus OH, United States of America
- 110 Faculty of Science, Okayama University, Okayama, Japan
- 111 Homer L. Dodge Department of Physics and Astronomy, University of Oklahoma, Norman OK, United States of America
- 112 Department of Physics, Oklahoma State University, Stillwater OK, United States of America
- 113 Palacký University, RCPTM, Olomouc, Czech Republic
- 114 Center for High Energy Physics, University of Oregon, Eugene OR, United States of America
- 115 LAL, Univ. Paris-Sud and CNRS/IN2P3, Orsay, France
- 116 Graduate School of Science, Osaka University, Osaka, Japan
- 117 Department of Physics, University of Oslo, Oslo, Norway
- 118 Department of Physics, Oxford University, Oxford, United Kingdom
- 119 ^(a)INFN Sezione di Pavia; ^(b)Dipartimento di Fisica, Università di Pavia, Pavia, Italy
- 120 Department of Physics, University of Pennsylvania, Philadelphia PA, United States of America
- 121 Petersburg Nuclear Physics Institute, Gatchina, Russia
- 122 ^(a)INFN Sezione di Pisa; ^(b)Dipartimento di Fisica E. Fermi, Università di Pisa, Pisa, Italy
- 123 Department of Physics and Astronomy, University of Pittsburgh, Pittsburgh PA, United States of America

America

- ¹²⁴ (a) Laboratório de Instrumentação e Física Experimental de Partículas - LIP, Lisboa, Portugal; (b) Departamento de Física Teórica y del Cosmos and CAFPE, Universidad de Granada, Granada, Spain
- ¹²⁵ Institute of Physics, Academy of Sciences of the Czech Republic, Praha, Czech Republic
- ¹²⁶ Faculty of Mathematics and Physics, Charles University in Prague, Praha, Czech Republic
- ¹²⁷ Czech Technical University in Prague, Praha, Czech Republic
- ¹²⁸ State Research Center Institute for High Energy Physics, Protvino, Russia
- ¹²⁹ Particle Physics Department, Rutherford Appleton Laboratory, Didcot, United Kingdom
- ¹³⁰ Physics Department, University of Regina, Regina SK, Canada
- ¹³¹ Ritsumeikan University, Kusatsu, Shiga, Japan
- ¹³² (a) INFN Sezione di Roma I; (b) Dipartimento di Fisica, Università La Sapienza, Roma, Italy
- ¹³³ (a) INFN Sezione di Roma Tor Vergata; (b) Dipartimento di Fisica, Università di Roma Tor Vergata, Roma, Italy
- ¹³⁴ (a) INFN Sezione di Roma Tre; (b) Dipartimento di Fisica, Università Roma Tre, Roma, Italy
- ¹³⁵ (a) Faculté des Sciences Ain Chock, Réseau Universitaire de Physique des Hautes Energies - Université Hassan II, Casablanca; (b) Centre National de l'Energie des Sciences Techniques Nucleaires, Rabat; (c) Faculté des Sciences Semlalia, Université Cadi Ayyad, LPHEA-Marrakech; (d) Faculté des Sciences, Université Mohamed Premier and LPTPM, Oujda; (e) Faculty of sciences, Mohammed V-Agdal University, Rabat, Morocco
- ¹³⁶ DSM/IRFU (Institut de Recherches sur les Lois Fondamentales de l'Univers), CEA Saclay (Commissariat a l'Energie Atomique), Gif-sur-Yvette, France
- ¹³⁷ Santa Cruz Institute for Particle Physics, University of California Santa Cruz, Santa Cruz CA, United States of America
- ¹³⁸ Department of Physics, University of Washington, Seattle WA, United States of America
- ¹³⁹ Department of Physics and Astronomy, University of Sheffield, Sheffield, United Kingdom
- ¹⁴⁰ Department of Physics, Shinshu University, Nagano, Japan
- ¹⁴¹ Fachbereich Physik, Universität Siegen, Siegen, Germany
- ¹⁴² Department of Physics, Simon Fraser University, Burnaby BC, Canada
- ¹⁴³ SLAC National Accelerator Laboratory, Stanford CA, United States of America
- ¹⁴⁴ (a) Faculty of Mathematics, Physics & Informatics, Comenius University, Bratislava; (b) Department of Subnuclear Physics, Institute of Experimental Physics of the Slovak Academy of Sciences, Kosice, Slovak Republic
- ¹⁴⁵ (a) Department of Physics, University of Johannesburg, Johannesburg; (b) School of Physics, University of the Witwatersrand, Johannesburg, South Africa
- ¹⁴⁶ (a) Department of Physics, Stockholm University; (b) The Oskar Klein Centre, Stockholm, Sweden
- ¹⁴⁷ Physics Department, Royal Institute of Technology, Stockholm, Sweden
- ¹⁴⁸ Departments of Physics & Astronomy and Chemistry, Stony Brook University, Stony Brook NY, United States of America
- ¹⁴⁹ Department of Physics and Astronomy, University of Sussex, Brighton, United Kingdom
- ¹⁵⁰ School of Physics, University of Sydney, Sydney, Australia
- ¹⁵¹ Institute of Physics, Academia Sinica, Taipei, Taiwan
- ¹⁵² Department of Physics, Technion: Israel Inst. of Technology, Haifa, Israel
- ¹⁵³ Raymond and Beverly Sackler School of Physics and Astronomy, Tel Aviv University, Tel Aviv, Israel
- ¹⁵⁴ Department of Physics, Aristotle University of Thessaloniki, Thessaloniki, Greece
- ¹⁵⁵ International Center for Elementary Particle Physics and Department of Physics, The University of Tokyo, Tokyo, Japan
- ¹⁵⁶ Graduate School of Science and Technology, Tokyo Metropolitan University, Tokyo, Japan
- ¹⁵⁷ Department of Physics, Tokyo Institute of Technology, Tokyo, Japan
- ¹⁵⁸ Department of Physics, University of Toronto, Toronto ON, Canada
- ¹⁵⁹ (a) TRIUMF, Vancouver BC; (b) Department of Physics and Astronomy, York University, Toronto ON, Canada
- ¹⁶⁰ Institute of Pure and Applied Sciences, University of Tsukuba, 1-1-1 Tennodai, Tsukuba, Ibaraki

305-8571, Japan

¹⁶¹ Science and Technology Center, Tufts University, Medford MA, United States of America

¹⁶² Centro de Investigaciones, Universidad Antonio Narino, Bogota, Colombia

¹⁶³ Department of Physics and Astronomy, University of California Irvine, Irvine CA, United States of America

¹⁶⁴ ^(a)INFN Gruppo Collegato di Udine; ^(b)ICTP, Trieste; ^(c)Dipartimento di Chimica, Fisica e Ambiente, Università di Udine, Udine, Italy

¹⁶⁵ Department of Physics, University of Illinois, Urbana IL, United States of America

¹⁶⁶ Department of Physics and Astronomy, University of Uppsala, Uppsala, Sweden

¹⁶⁷ Instituto de Física Corpuscular (IFIC) and Departamento de Física Atómica, Molecular y Nuclear and Departamento de Ingeniería Electrónica and Instituto de Microelectrónica de Barcelona (IMB-CNM), University of Valencia and CSIC, Valencia, Spain

¹⁶⁸ Department of Physics, University of British Columbia, Vancouver BC, Canada

¹⁶⁹ Department of Physics and Astronomy, University of Victoria, Victoria BC, Canada

¹⁷⁰ Department of Physics, University of Warwick, Coventry, United Kingdom

¹⁷¹ Waseda University, Tokyo, Japan

¹⁷² Department of Particle Physics, The Weizmann Institute of Science, Rehovot, Israel

¹⁷³ Department of Physics, University of Wisconsin, Madison WI, United States of America

¹⁷⁴ Fakultät für Physik und Astronomie, Julius-Maximilians-Universität, Würzburg, Germany

¹⁷⁵ Fachbereich C Physik, Bergische Universität Wuppertal, Wuppertal, Germany

¹⁷⁶ Department of Physics, Yale University, New Haven CT, United States of America

¹⁷⁷ Yerevan Physics Institute, Yerevan, Armenia

¹⁷⁸ Domaine scientifique de la Doua, Centre de Calcul CNRS/IN2P3, Villeurbanne Cedex, France

^a Also at Laboratório de Instrumentação e Física Experimental de Partículas - LIP, Lisboa, Portugal

^b Also at Faculdade de Ciências and CFNUL, Universidade de Lisboa, Lisboa, Portugal

^c Also at Particle Physics Department, Rutherford Appleton Laboratory, Didcot, United Kingdom

^d Also at TRIUMF, Vancouver BC, Canada

^e Also at Department of Physics, California State University, Fresno CA, United States of America

^f Also at Novosibirsk State University, Novosibirsk, Russia

^g Also at Fermilab, Batavia IL, United States of America

^h Also at Department of Physics, University of Coimbra, Coimbra, Portugal

ⁱ Also at Università di Napoli Parthenope, Napoli, Italy

^j Also at Institute of Particle Physics (IPP), Canada

^k Also at Department of Physics, Middle East Technical University, Ankara, Turkey

^l Also at Louisiana Tech University, Ruston LA, United States of America

^m Also at Department of Physics and Astronomy, University College London, London, United Kingdom

ⁿ Also at Group of Particle Physics, University of Montreal, Montreal QC, Canada

^o Also at Department of Physics, University of Cape Town, Cape Town, South Africa

^p Also at Institute of Physics, Azerbaijan Academy of Sciences, Baku, Azerbaijan

^q Also at Institut für Experimentalphysik, Universität Hamburg, Hamburg, Germany

^r Also at Manhattan College, New York NY, United States of America

^s Also at School of Physics, Shandong University, Shandong, China

^t Also at CPPM, Aix-Marseille Université and CNRS/IN2P3, Marseille, France

^u Also at School of Physics and Engineering, Sun Yat-sen University, Guanzhou, China

^v Also at Academia Sinica Grid Computing, Institute of Physics, Academia Sinica, Taipei, Taiwan

^w Also at Dipartimento di Fisica, Università La Sapienza, Roma, Italy

^x Also at DSM/IRFU (Institut de Recherches sur les Lois Fondamentales de l'Univers), CEA Saclay (Commissariat à l'Energie Atomique), Gif-sur-Yvette, France

^y Also at Section de Physique, Université de Genève, Geneva, Switzerland

^z Also at Departamento de Física, Universidade de Minho, Braga, Portugal

^{aa} Also at Department of Physics and Astronomy, University of South Carolina, Columbia SC, United States of America

^{ab} Also at Institute for Particle and Nuclear Physics, Wigner Research Centre for Physics, Budapest, Hungary

^{ac} Also at California Institute of Technology, Pasadena CA, United States of America

^{ad} Also at Institute of Physics, Jagiellonian University, Krakow, Poland

^{ae} Also at LAL, Univ. Paris-Sud and CNRS/IN2P3, Orsay, France

^{af} Also at Department of Physics and Astronomy, University of Sheffield, Sheffield, United Kingdom

^{ag} Also at Department of Physics, Oxford University, Oxford, United Kingdom

^{ah} Also at Institute of Physics, Academia Sinica, Taipei, Taiwan

^{ai} Also at Department of Physics, The University of Michigan, Ann Arbor MI, United States of America

* Deceased